

Testing primordial non-Gaussianity with CMB and LSS data.

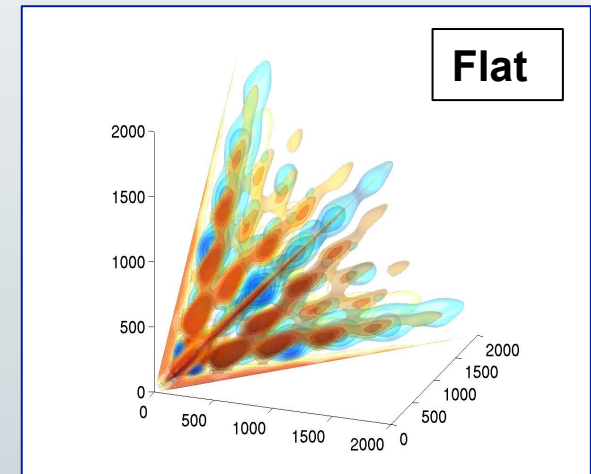
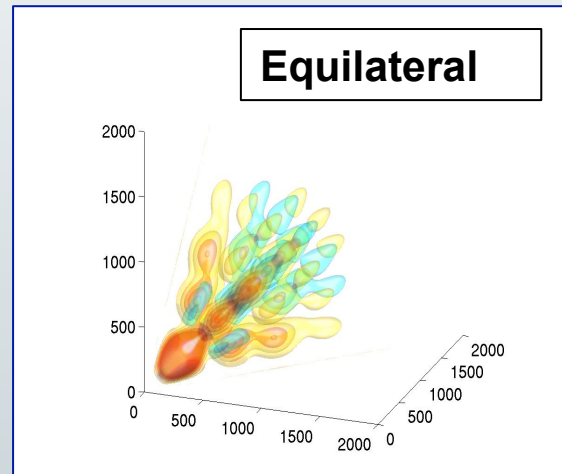
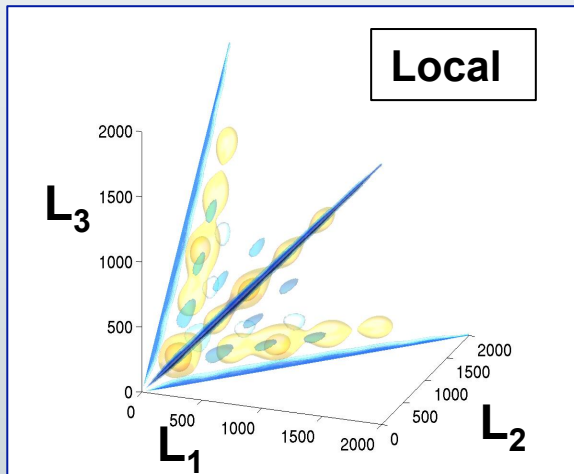
Michele Liguori

Department of Physics and Astronomy,

University of Padova

Beyond power spectra: non-Gaussianity

Primordial non-Gaussianity. Many inflationary scenarios (notably, multi-field Inflation) predict small, model-dependent deviations from Gaussianity. **Additional information in 3-point (bispectrum) and 4-point (trispectrum) correlation functions.**



- Fit primordial bispectrum (trispectrum) template to the data and measure the degree of correlation via a dimensionless parameter f_{NL} (g_{NL} , τ_{NL}).
- Large f_{NL} for a given shape selects specific scenarios. E.g. **large local f_{NL} would rule out standard single-field models.**

Primordial and CMB bispectrum

Non-Gaussianity: higher order correlators of the primordial curvature perturbation field are non-vanishing

- Largest correlator (in most cases): the primordial bispectrum

Primordial and CMB bispectrum

Non-Gaussianity: higher order correlators of the primordial curvature perturbation field are non-vanishing

- Largest correlator (in most cases): the primordial bispectrum

$$\langle \Phi(k_1) \Phi(k_2) \Phi(k_3) \rangle = (2\pi)^3 F(k_1, k_2, k_3) \delta(\vec{k}_1 + \vec{k}_2 + \vec{k}_3)$$

$f_{NL} \equiv \frac{k^6 F(k, k, k)}{6\Delta_\Phi^2(k)}$

Amplitude

Primordial potential

Shape

Translation invariance

Primordial and CMB bispectrum

Non-Gaussianity: higher order correlators of the primordial curvature perturbation field are non-vanishing

- Largest correlator (in most cases): the primordial bispectrum

$$\langle \Phi(k_1) \Phi(k_2) \Phi(k_3) \rangle = (2\pi)^3 F(k_1, k_2, k_3) \delta(\vec{k}_1 + \vec{k}_2 + \vec{k}_3)$$

$f_{NL} \equiv \frac{k^6 F(k, k, k)}{6\Delta_\Phi^2(k)}$

Amplitude Primordial potential Shape Translation invariance

- What we measure is the CMB angular bispectrum :

$$B_{\ell_1 \ell_2 \ell_3}^{m_1 m_2 m_3} = \langle a_{\ell_1}^{m_1} a_{\ell_2}^{m_2} a_{\ell_3}^{m_3} \rangle$$

Primordial and CMB bispectrum

Non-Gaussianity: higher order correlators of the primordial curvature perturbation field are non-vanishing

- Largest correlator (in most cases): the primordial bispectrum

$$\langle \Phi(k_1) \Phi(k_2) \Phi(k_3) \rangle = (2\pi)^3 F(k_1, k_2, k_3) \delta(\vec{k}_1 + \vec{k}_2 + \vec{k}_3)$$

$f_{NL} \equiv \frac{k^6 F(k, k, k)}{6\Delta_\Phi^2(k)}$

Amplitude

Primordial potential

Shape

Translation invariance

- What we measure is the CMB angular bispectrum :

$$B_{\ell_1 \ell_2 \ell_3}^{m_1 m_2 m_3} = \langle a_{\ell_1}^{m_1} a_{\ell_2}^{m_2} a_{\ell_3}^{m_3} \rangle$$

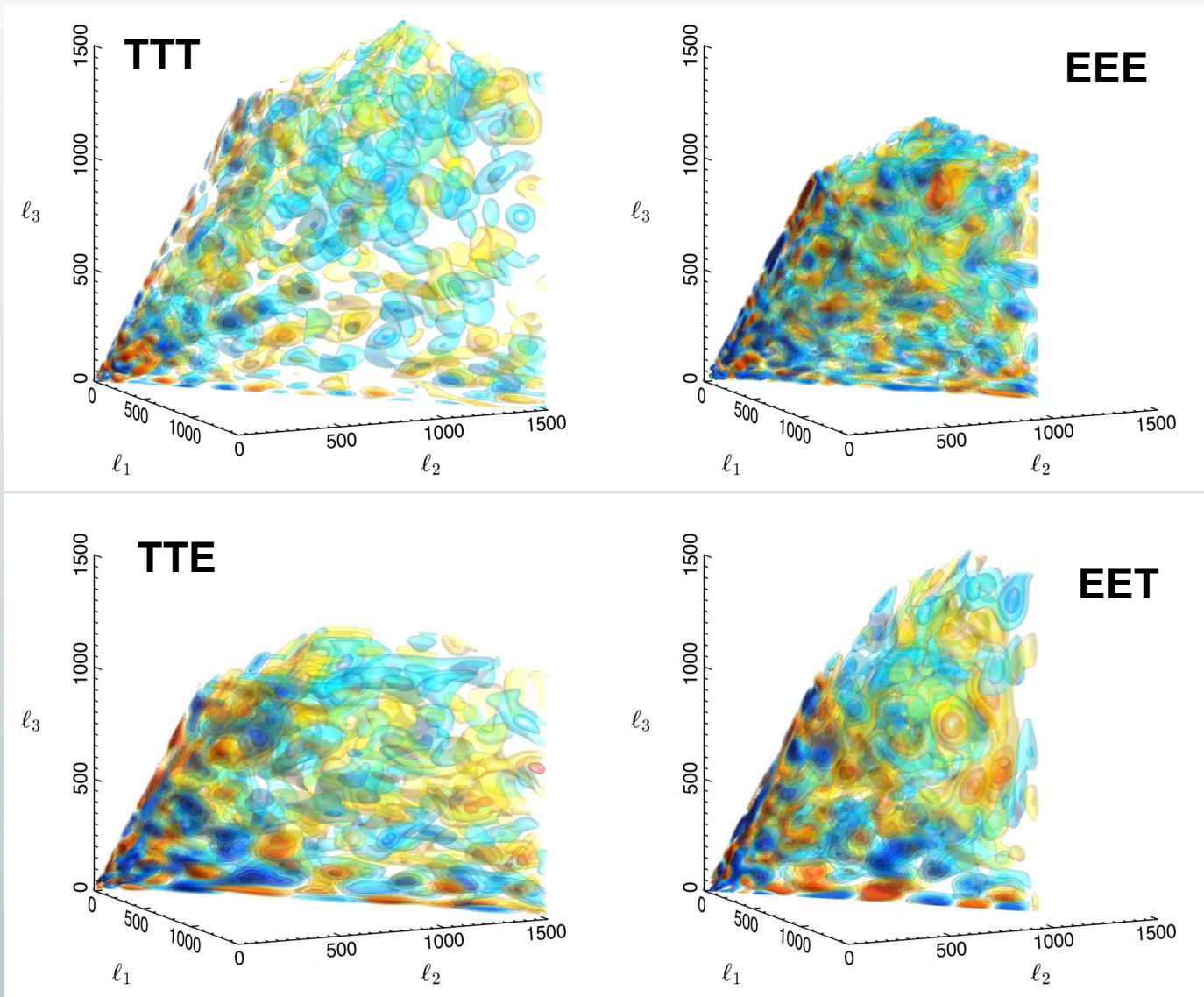
- Primordial and CMB bispectra are linked through linear radiative transfer effects (same as for power spectrum)

The scientific results that we present today are a product of the Planck Collaboration, including individuals from more than 100 scientific institutes in Europe, the USA and Canada



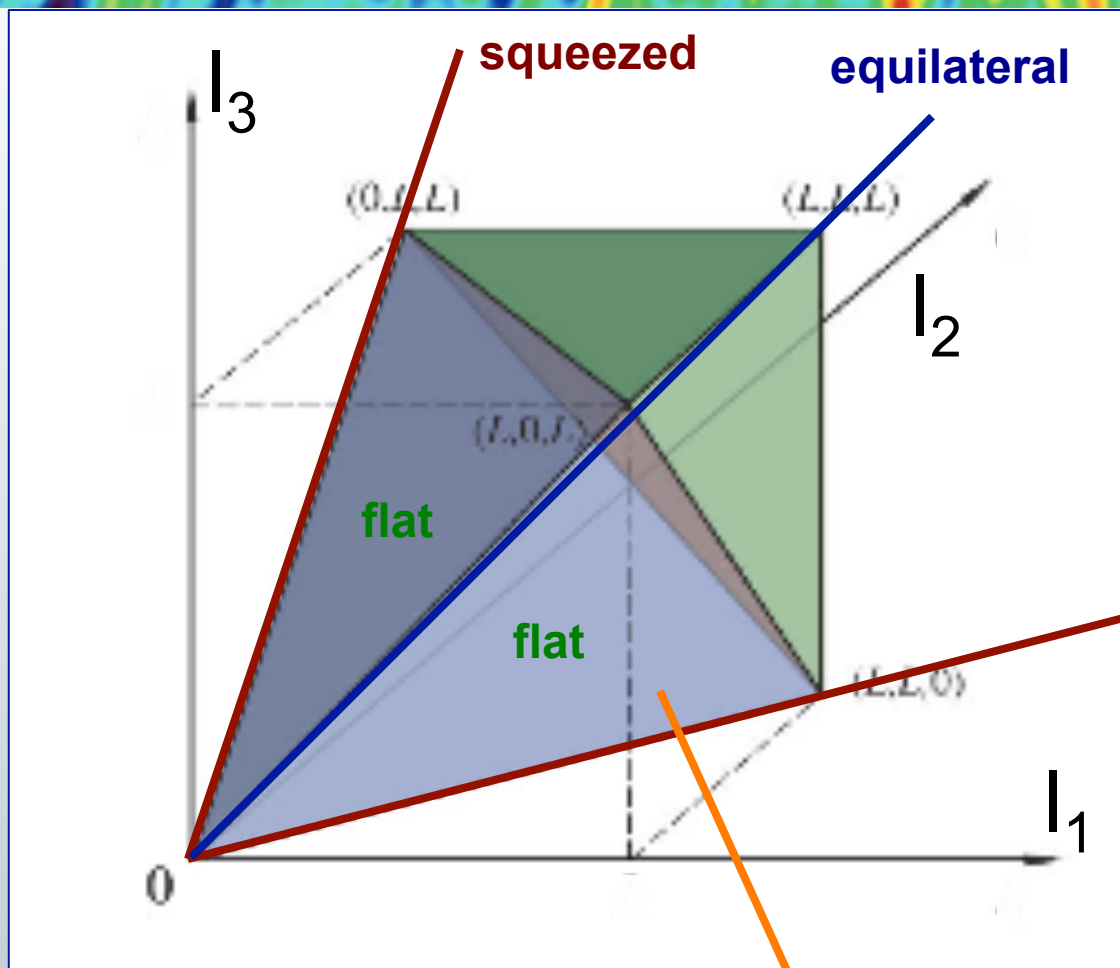
Planck is a project of the European Space Agency, with instruments provided by two scientific Consortia funded by ESA member states (in particular the lead countries: France and Italy) with contributions from NASA (USA), and telescope reflectors provided in a collaboration between ESA and a scientific Consortium led and funded by Denmark.

The 2015 *Planck* bispectrum (modal)



(S/N
weighted)

Bispectrum



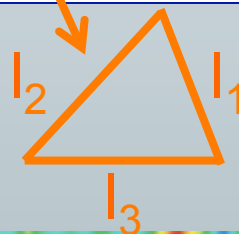
$$l_1 \sim l_2 \sim l_3$$



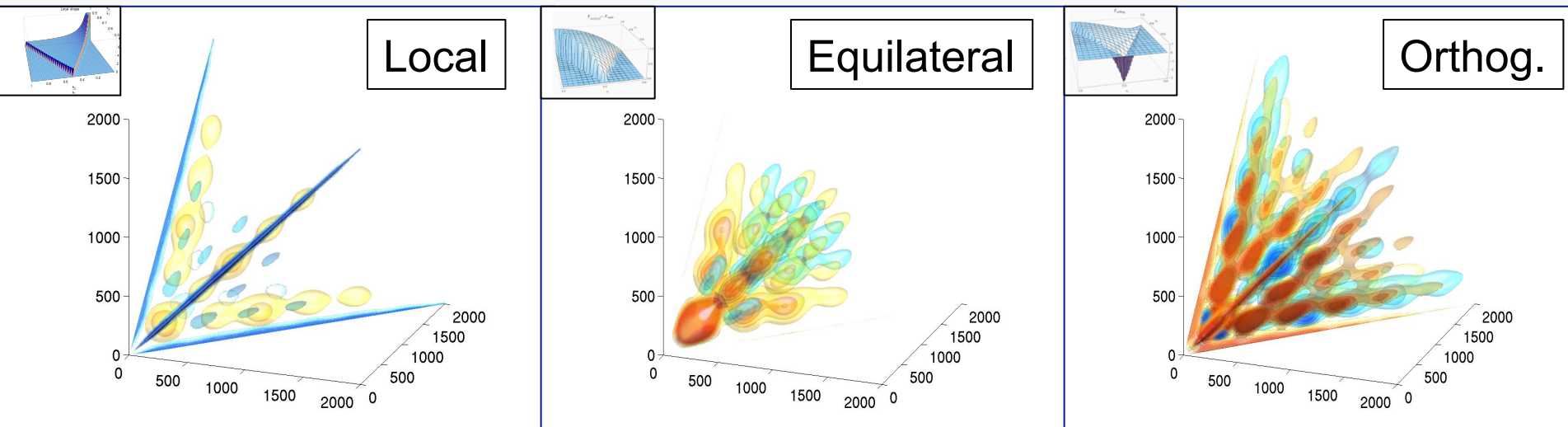
$$l_1 \ll l_2, l_3$$



$$l_2 \sim l_3$$

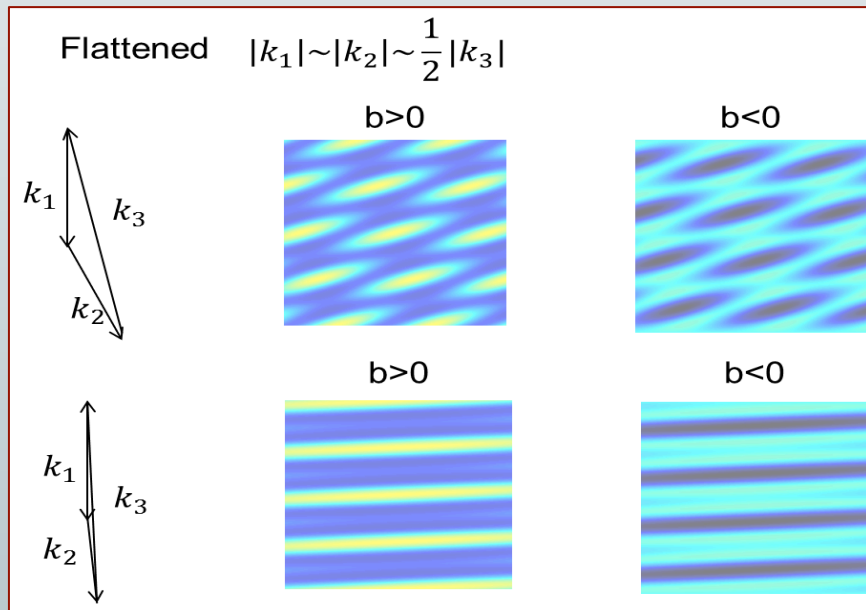
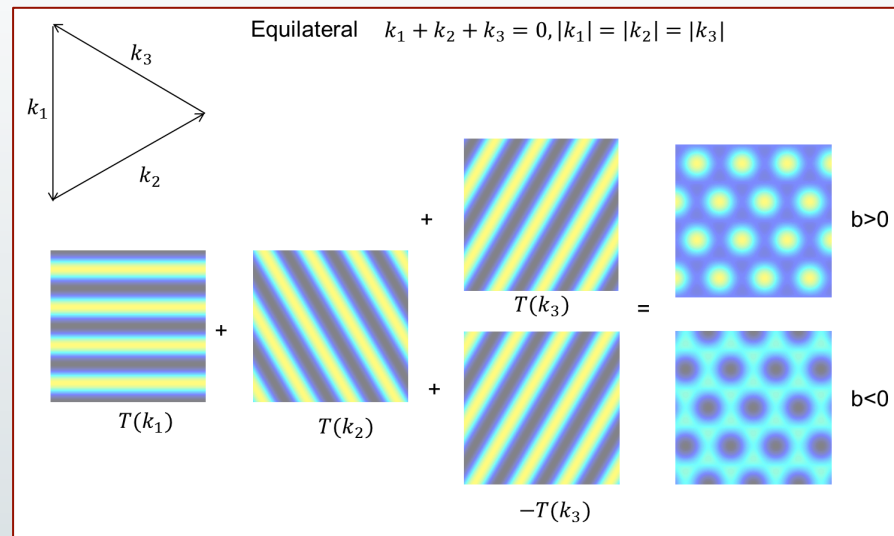
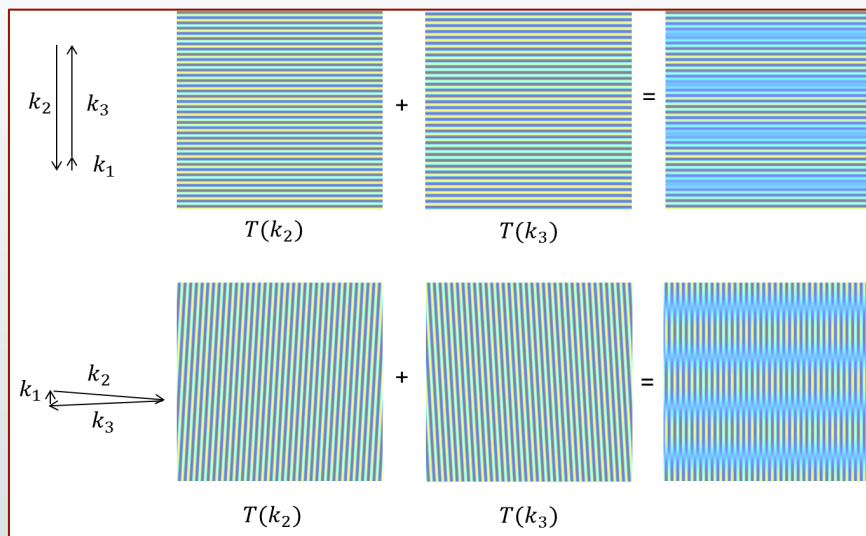


Main primordial shapes



- Local shape: peaked on squeezed triangles. Multifield Inflation and Ekpyrotic models.
- Equilateral shape: single-field models with non-standard kinetic/higher-derivative terms, effective field theory
- Flat shape: linear combination of equilateral. and orthogonal. Non bunch Davies vacuum
- *Standard single field slow-roll: negligible NG (given current sensitivity)*

NG fields in real space



Local: large scale modulation of small scale power (more/less small scale structure in large scale overdense regions)

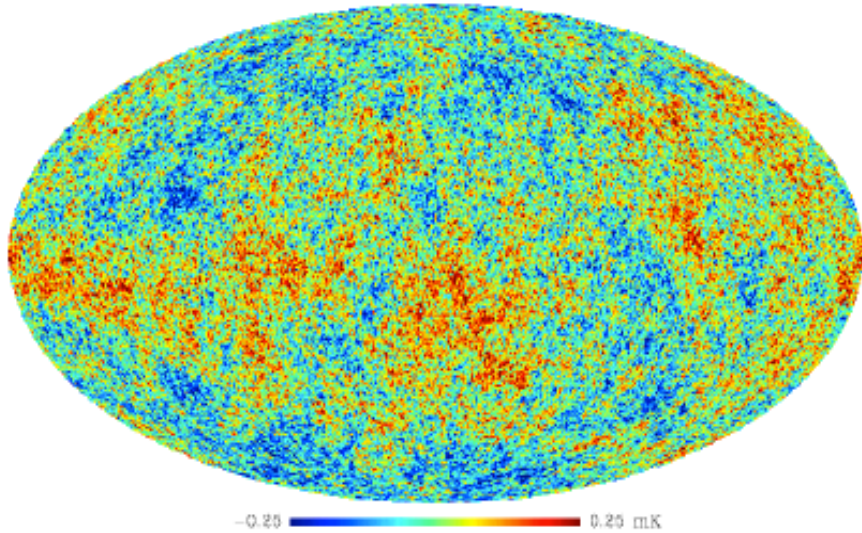
Equilateral: filamentary structure of over/underdense regions

Flattened: pancake structure

Lewis 2012

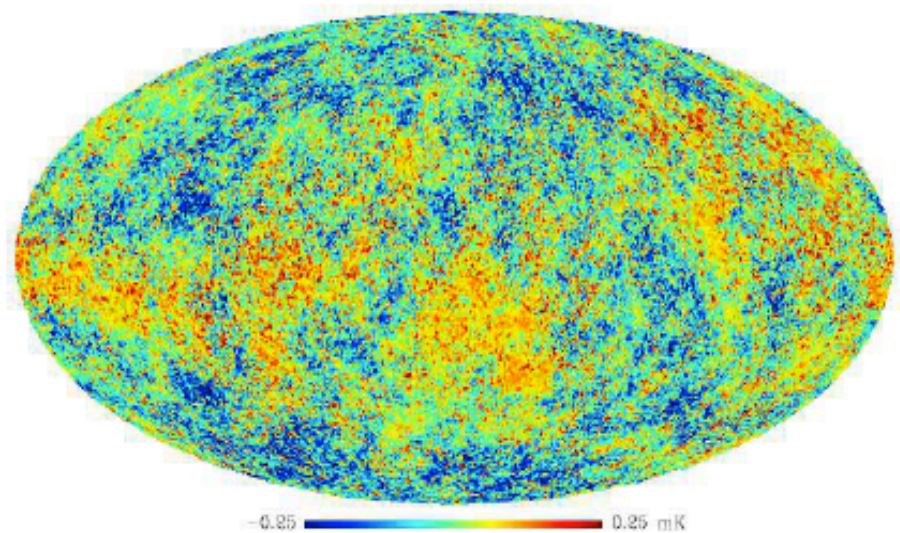
CMB local-type NG simulations

$$\Phi(\vec{x}) = \Phi_L(\vec{x}) + f_{NL} \left(\Phi_L^2(\vec{x}) - \langle \Phi^2(\vec{x}) \rangle \right) + g_{NL} \Phi_L^3(\vec{x})$$



Liguori et al. 2007

$$f_{NL} = 0, g_{NL} = 0$$



$$f_{NL} = 3000, g_{NL} = 0$$

Optimal f_{NL} bispectrum estimator

$$\hat{f}_{NL} = \frac{1}{N} \sum B_{\ell_1 \ell_2 \ell_3}^{m_1 m_2 m_3} (C^{-1}a)_{\ell_1}^{m_1} (C^{-1}a)_{\ell_2}^{m_2} (C^{-1}a)_{\ell_3}^{m_3} - 3C_{\ell_1 m_1 \ell_2 m_2}^{-1} (C^{-1}a)_{\ell_3}^{m_3}$$

Leaving aside complications coming from breaking of statistical isotropy (sky-cut, noise...), one can see that we are extracting the three point Function from the data and fitting theoretical bispectrum templates to it

$$\hat{f}_{NL} = \frac{1}{N} \sum_{\ell_i m_i} B_{\ell_1 \ell_2 \ell_3}^{m_1 m_2 m_3} \frac{a_{\ell_1}^{m_1}}{C_{\ell_1}} \frac{a_{\ell_2}^{m_2}}{C_{\ell_2}} \frac{a_{\ell_3}^{m_3}}{C_{\ell_3}}$$

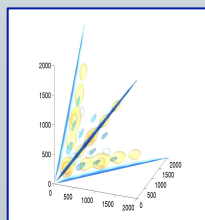
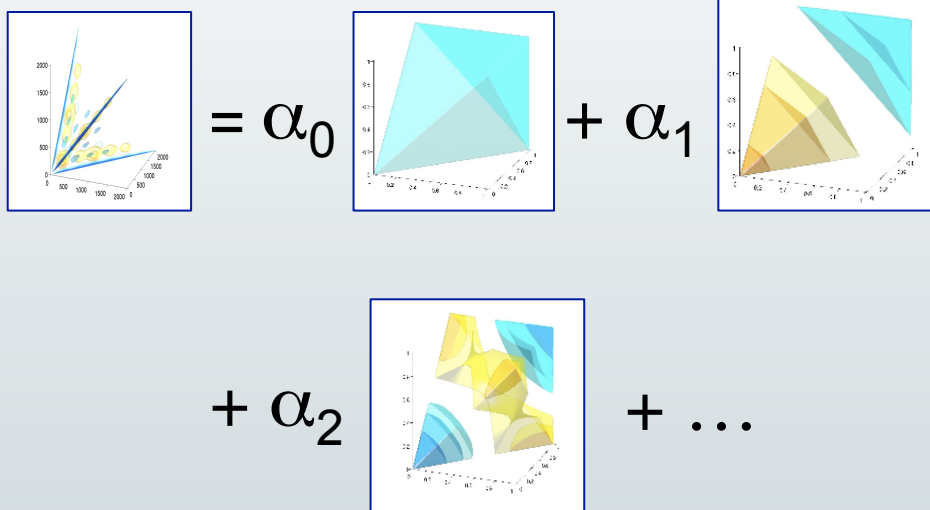
A brute force implementation scales like ℓ_{\max}^5 . Unfeasible at Planck (or WMAP) resolution.

Can achieve massive speed improvement (ℓ_{\max}^3 scaling) if the reduced bispectrum is *separable* (Komatsu, Spergel, Wandelt 2003). KSW method.

$$b_{\ell_1 \ell_2 \ell_3} = \sum_{ijk} X_{\ell_1}^i Y_{\ell_2}^j Z_{\ell_3}^k \Rightarrow B_{\ell_1 \ell_2 \ell_3}^{m_1 m_2 m_3} = b_{\ell_1 \ell_2 \ell_3} \int Y_{\ell_1}^{m_1}(\Omega) Y_{\ell_2}^{m_2}(\Omega) Y_{\ell_3}^{m_3}(\Omega)$$

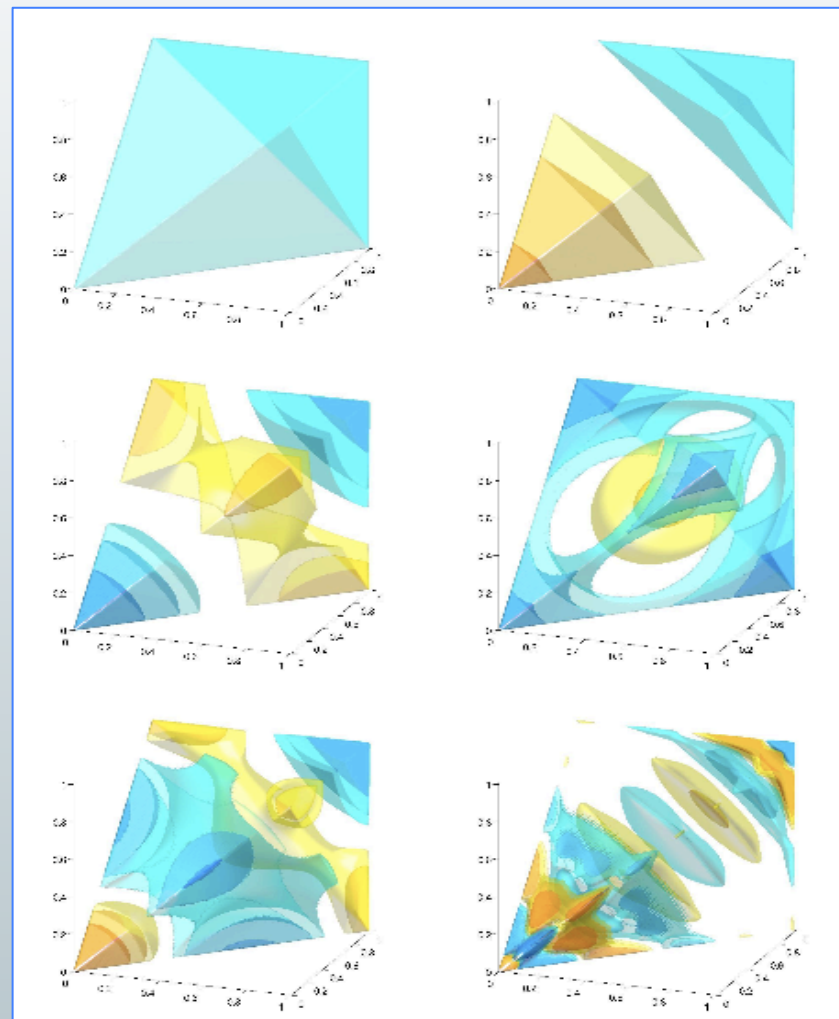
Modal expansion in figures

Expansion

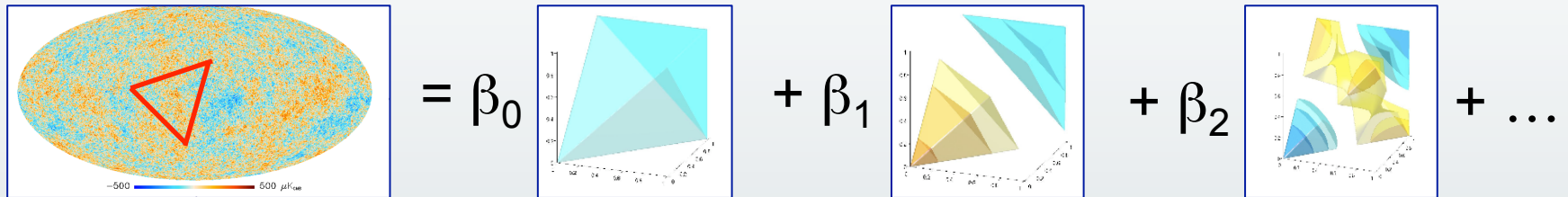


$$\rightarrow (\alpha_0, \alpha_1, \dots, \alpha_n)$$

Basis modes



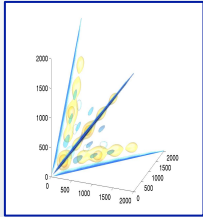
Bispectrum estimation



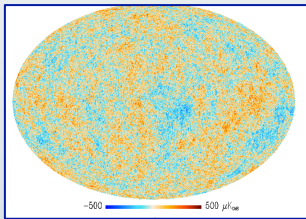
For a given dataset, extract best-fit β_i , $i=1,\dots,n$

- The basis elements pictured on the right *are by construction factorizable*
- Apply position space cubic statistics, KSW, to each separable template on the right to estimate the amplitudes β_i
- Orthonormal basis $\Rightarrow \beta_i$ uncorrelated (in first approx.)

f_{NL} and bispectrum reconstruction



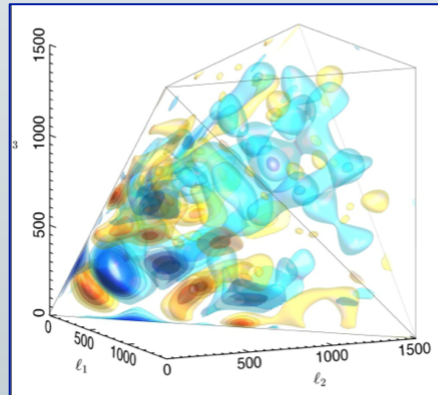
➔ $(\alpha_0, \alpha_1, \dots, \alpha_n)$ Theory



➔ $(\beta_0, \beta_1, \dots, \beta_n)$ Data
("mode spectrum")

$$f_{NL} = \frac{1}{N} \sum_n \alpha_n \beta_n$$

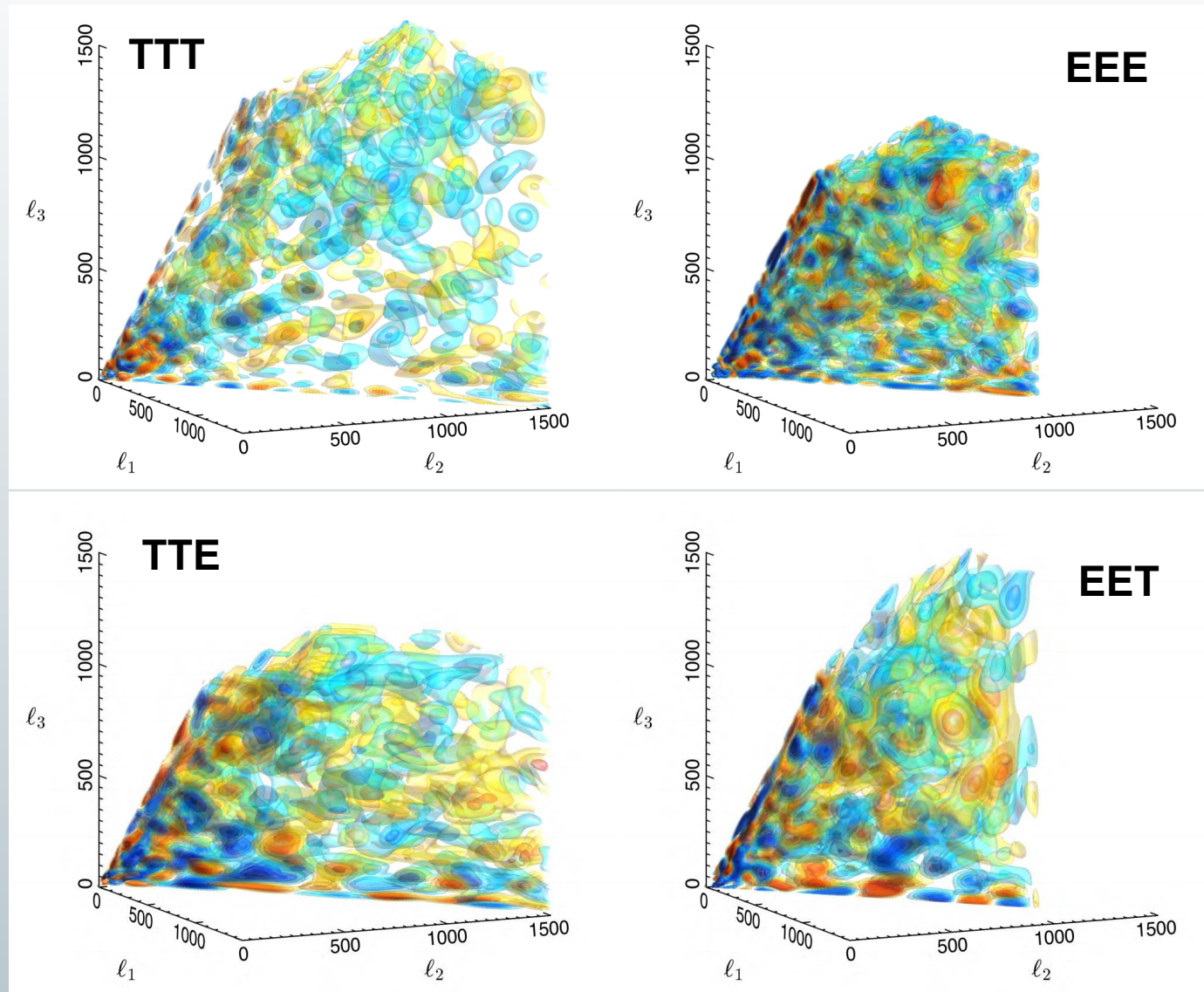
$$N = \frac{1}{6} \sum_n \alpha_n^2$$



$$= \sum_n \beta_n \mathfrak{R}_n$$

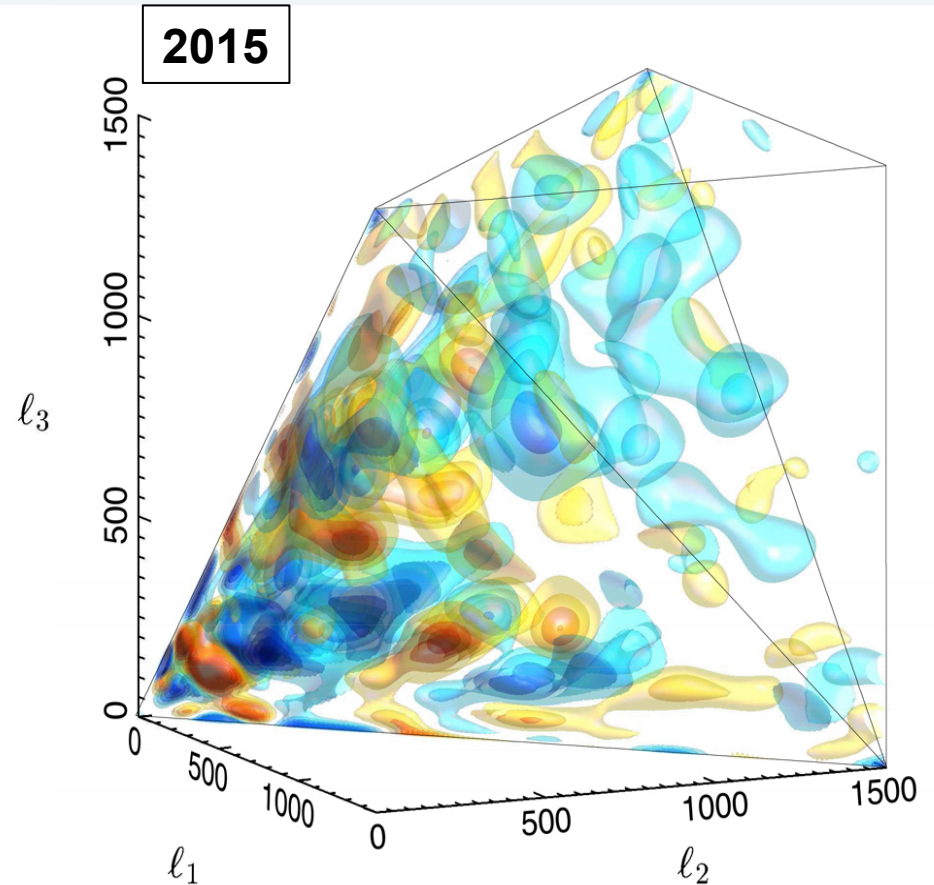
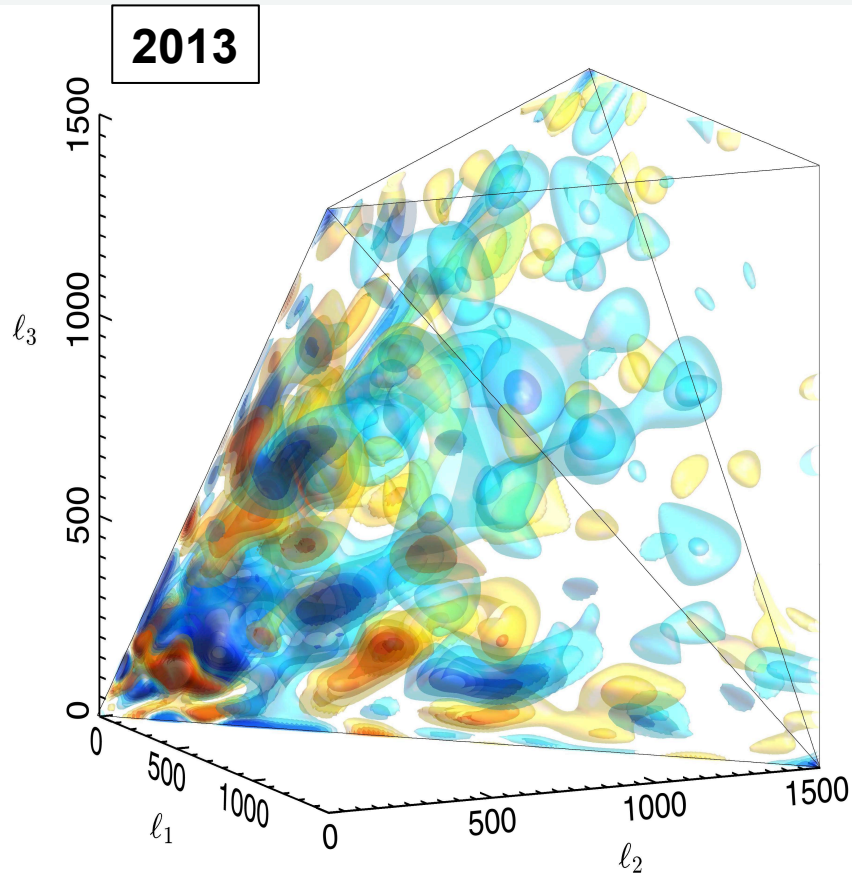
J. Fergusson, ML, P. Shellard 2009, 2010, arXiv: 0912.5516, 1006.1642
 J. Fergusson, P. Shellard, 2011, arXiv: 1105.2791,
 M. Shiraishi, ML, J. Fergusson 2014, arXiv: 1403.4222, 1409.0265
 J. Fergusson 2014, arXiv:1403.7949

The 2014 *Planck* bispectrum (modal)



(S/N
weighted)

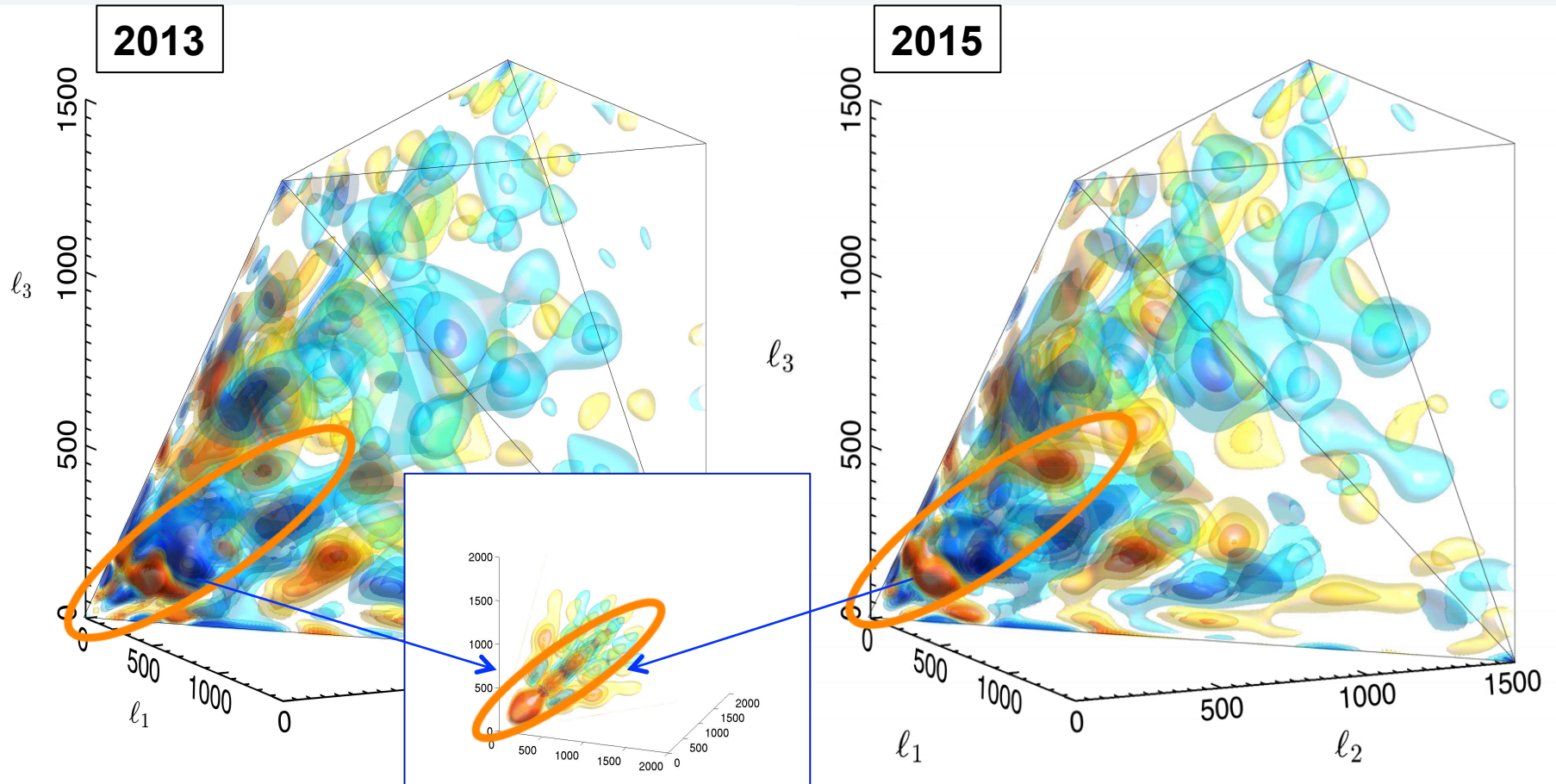
Planck TTT: 2013 vs Planck 2015



**Primordial NG Planck results:
Ade et al., Planck 2015 results. XVII**

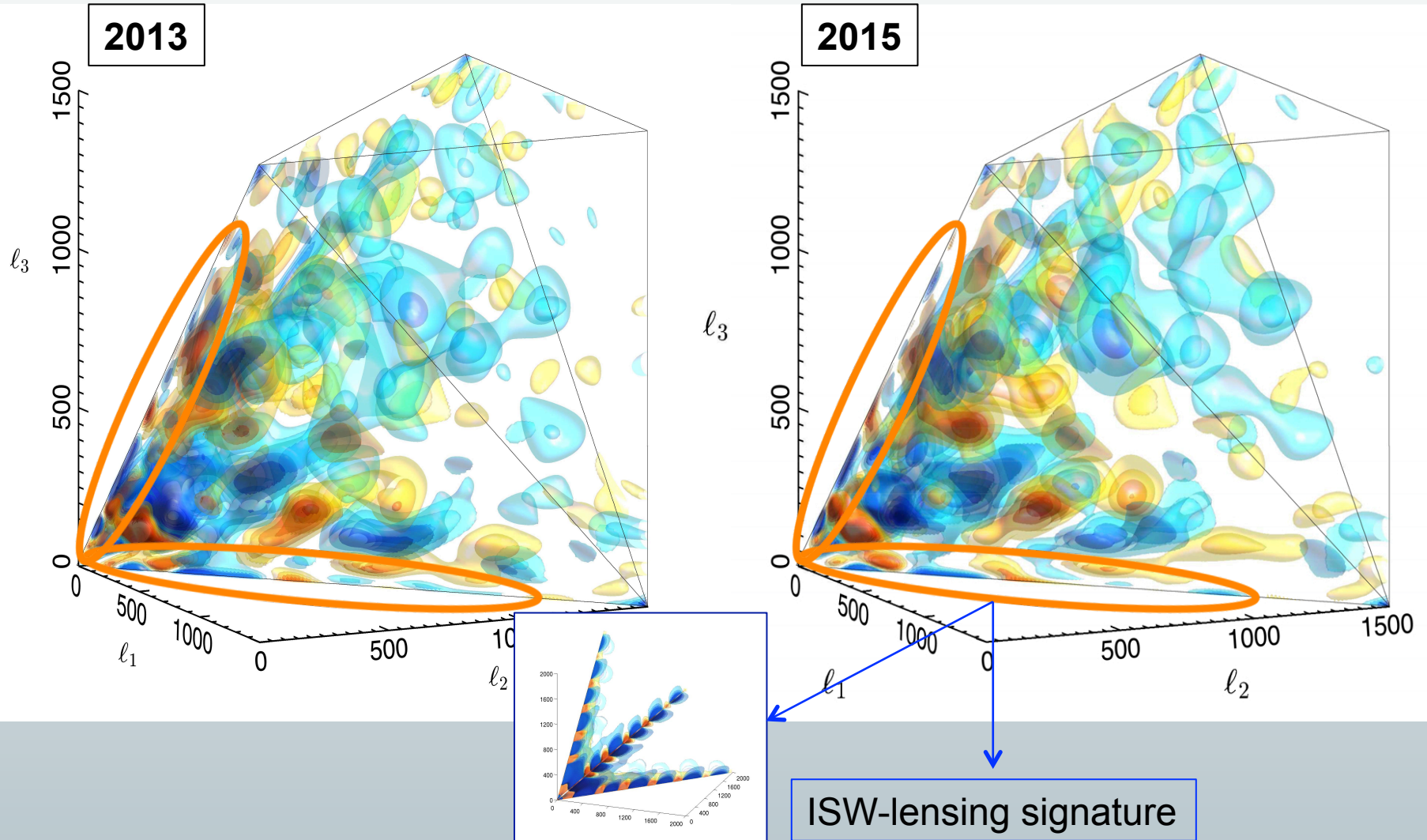
**Modal bispectrum reconstruction:
Fergusson, ML, Shellard 2010, 2011**

Planck TTT: 2013 vs Planck 2015



Does not match period of acoustic oscillations for primordial bispectra

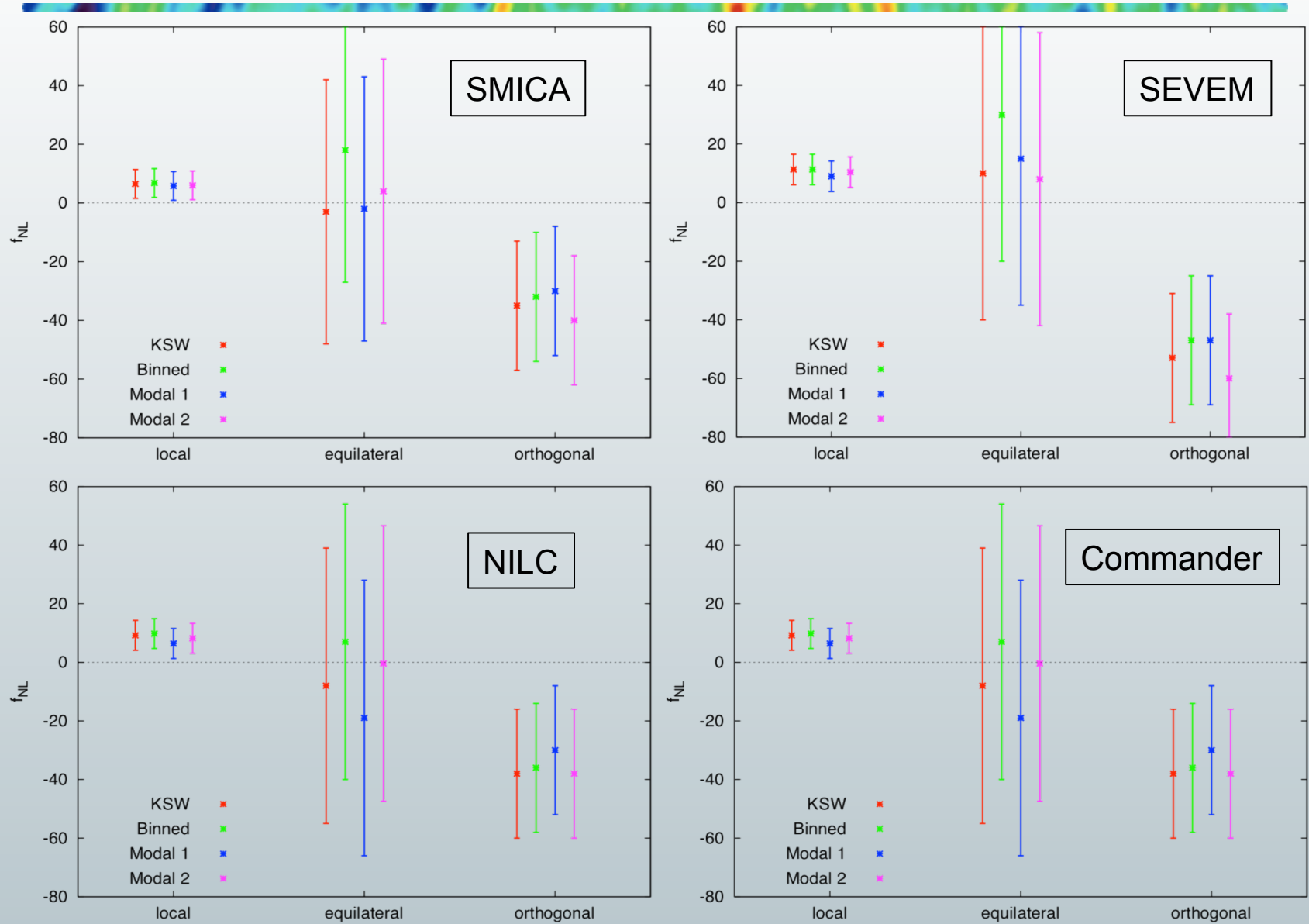
Planck TTT: 2013 vs Planck 2015



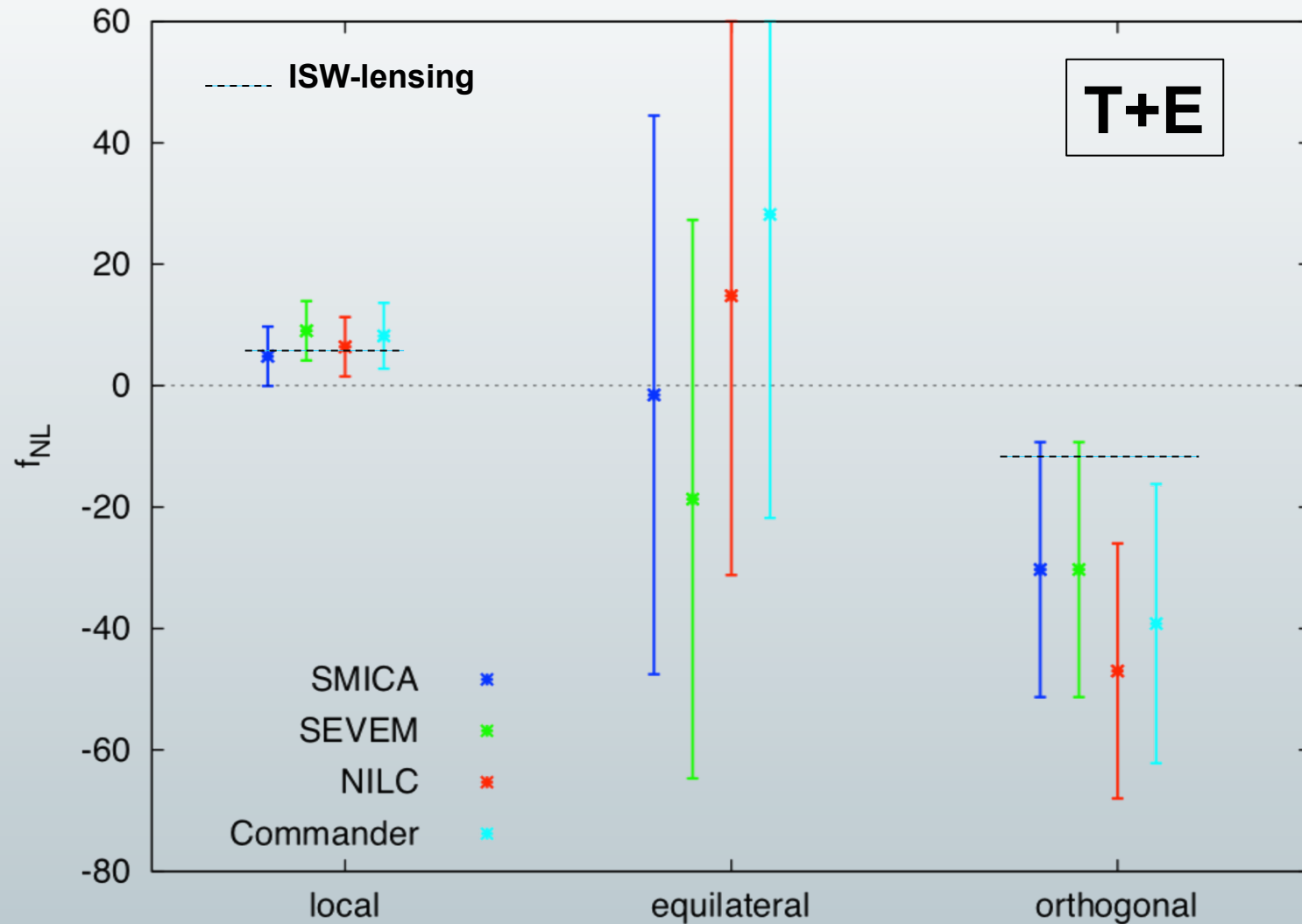
f_{NL} from *Planck* bispectrum (KSW)

$f_{\text{NL}}(\text{KSW})$		
Shape and method	Independent	ISW-lensing subtracted
SMICA (T)		
Local	10.2 \pm 5.7	2.5 \pm 5.7
Equilateral	−13 \pm 70	−16 \pm 70
Orthogonal	−56 \pm 33	−34 \pm 33
SMICA ($T+E$)		
Local	6.5 \pm 5.0	0.8 \pm 5.0
Equilateral	3 \pm 43	−4 \pm 43
Orthogonal	−36 \pm 21	−26 \pm 21

f_{NL} , estimators comparison



f_{NL} , cleaned maps comparison (modal)



Beyond “standard” shapes

- We compute f_{NL} for a large number of primordial models beyond the standard local, equilateral, orthogonal shapes, including
 - ✓ Equilateral family (DBI, EFT, ghost)
 - ✓ Flattened shapes (non-Bunch Davies)
 - ✓ Feature models (oscillatory bispectra, scale-dependent)
 - ✓ Direction dependence
 - ✓ Quasi-single-field
 - ✓ Parity-odd models
- **No evidence for NG found, constraints on parameters from the models above**
- **Extended survey of feature models with respect to 2013, 600 -> 2000 modes, including polarization.**

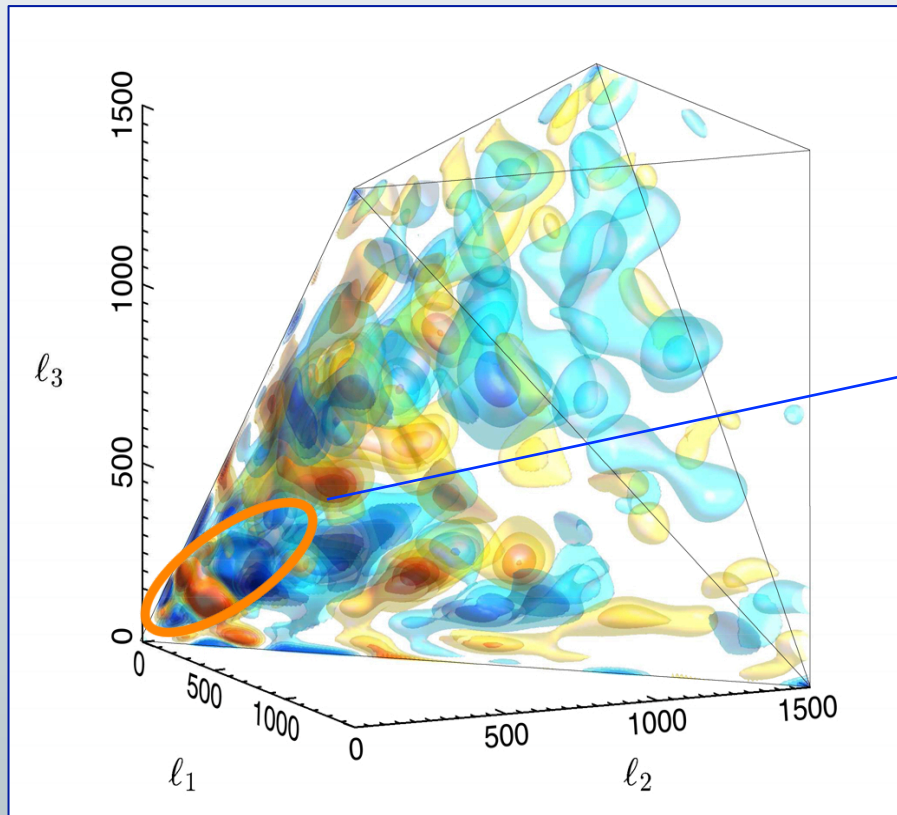
All primordial NG *Planck* results in ***Planck* 2015 results. XVII.**

Feature models

$$S \sim f_{NL}^{feat.} \sin\left(\frac{K}{k_*} + \phi\right)$$

$$S_{flat-feat.} = S_{flat} \times S_{feat}$$

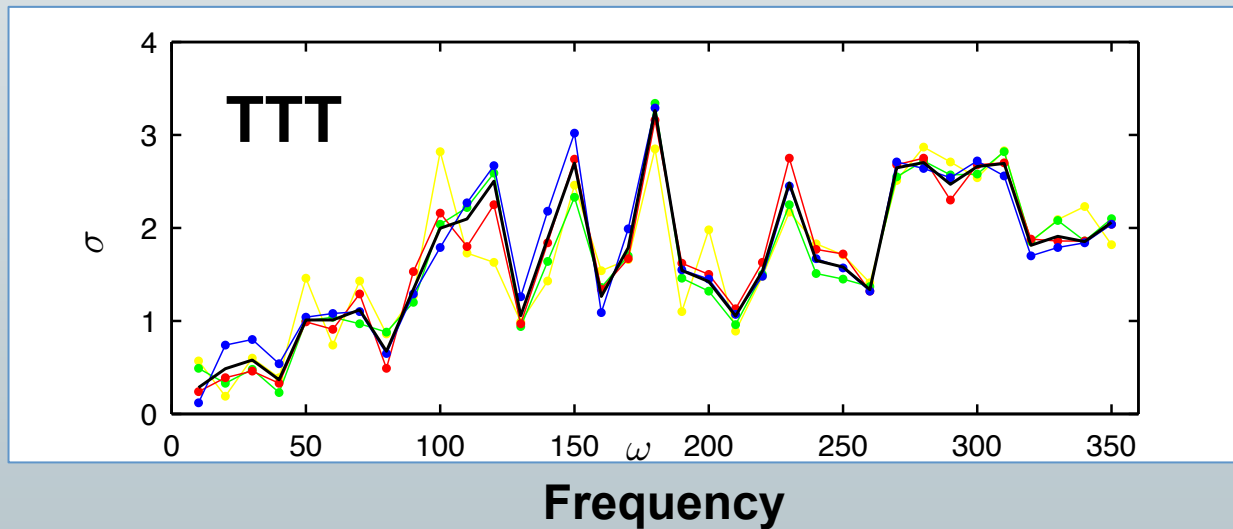
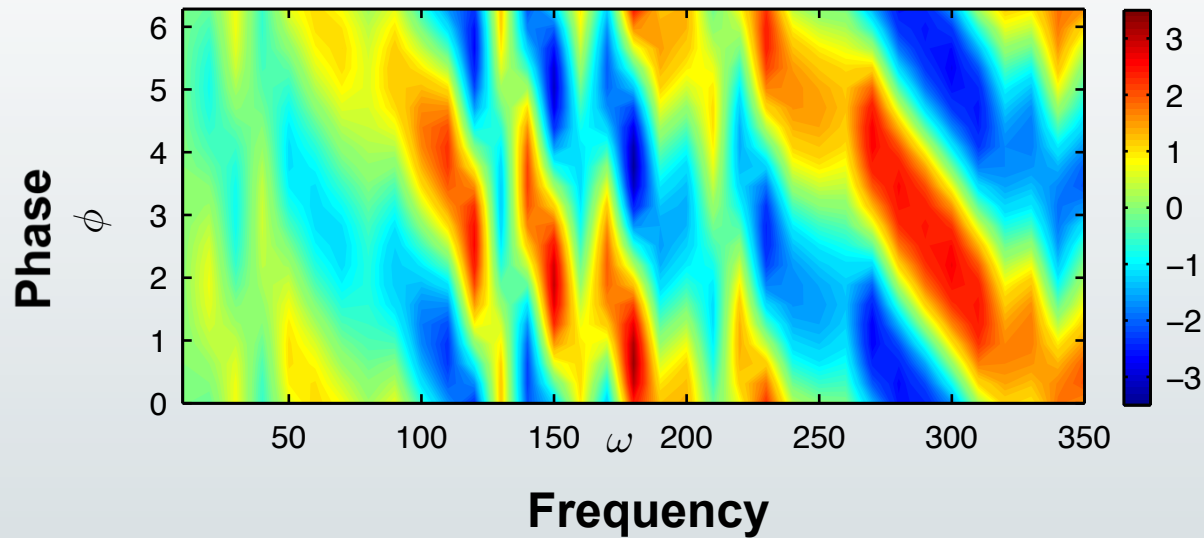
$$S_{equil-feat} = S_{equil} \times S_{feat}$$



Change of sign does not match acoustic peak

Can be captured by oscillating features

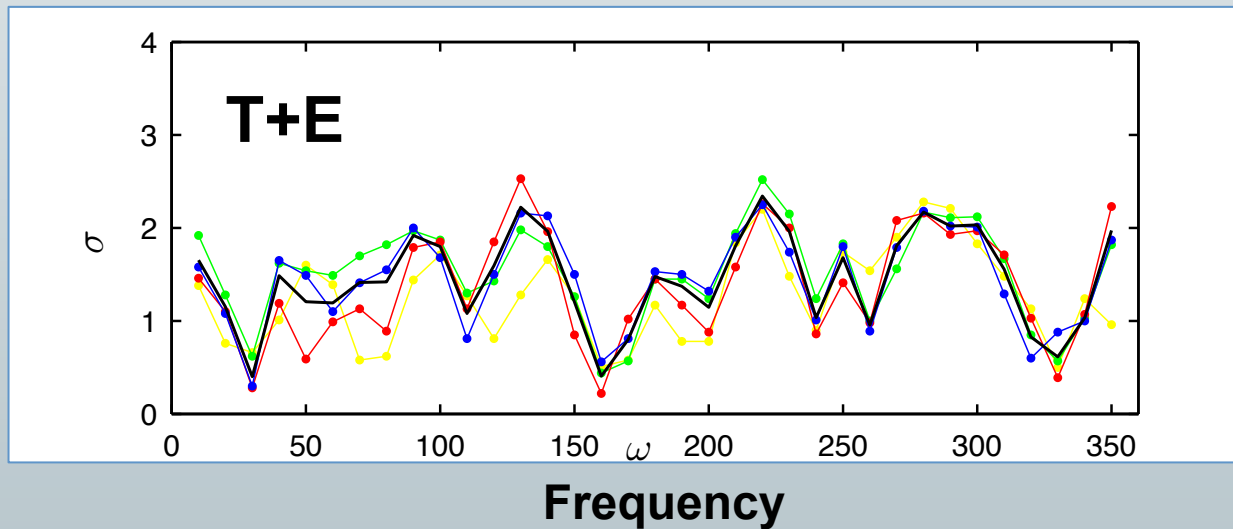
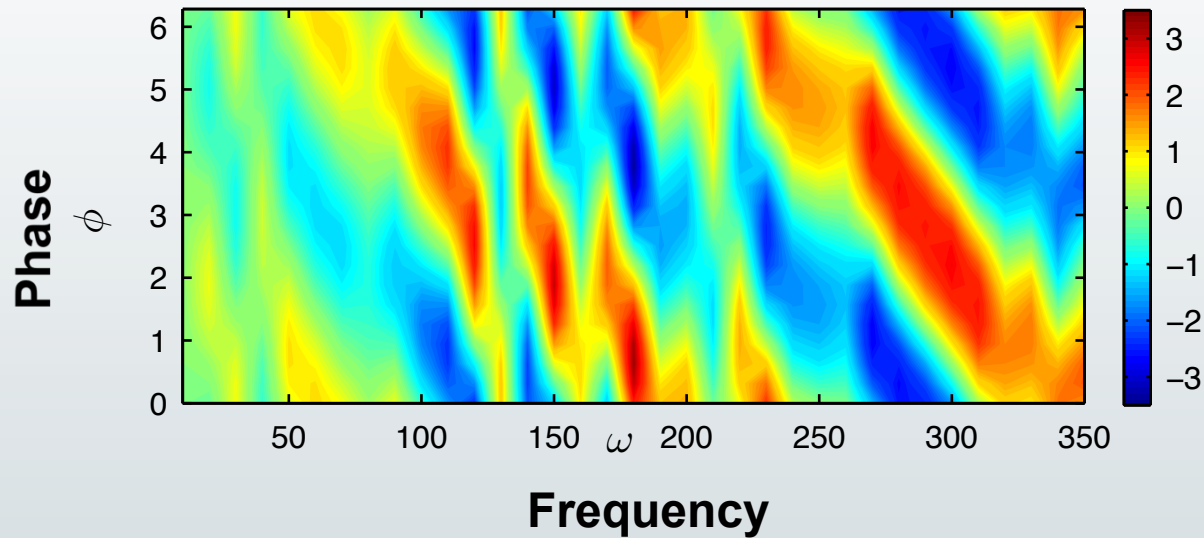
Features x Equilateral



Marginalizing over
phase

“Look elsewhere”
accounted for

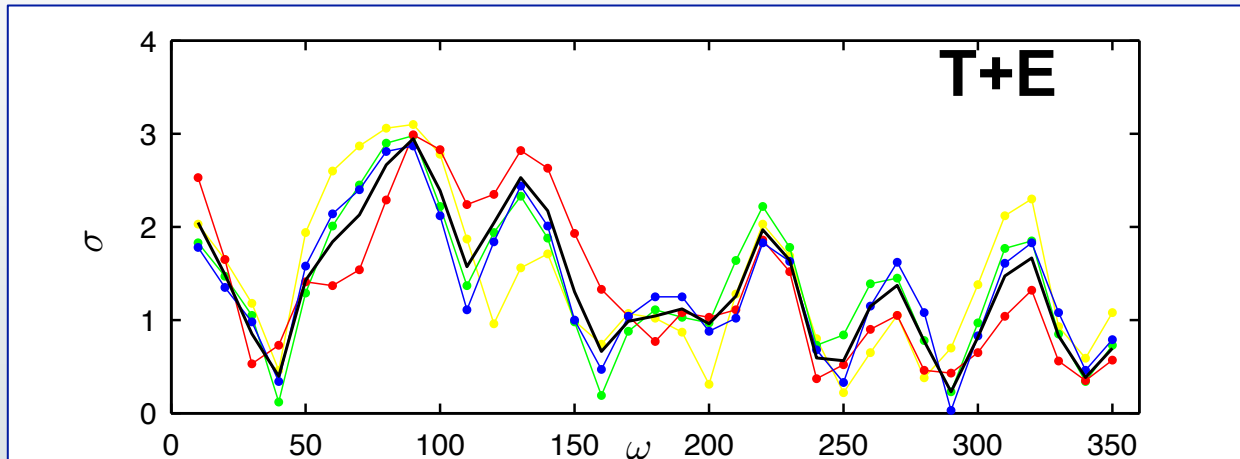
Features x Equilateral



Marginalizing over
phase

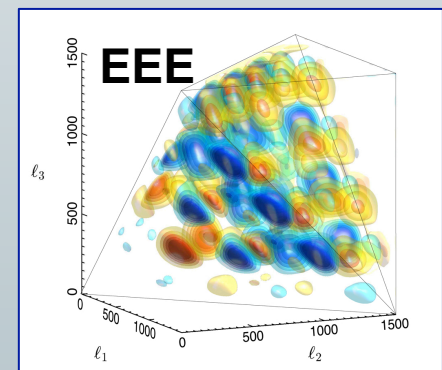
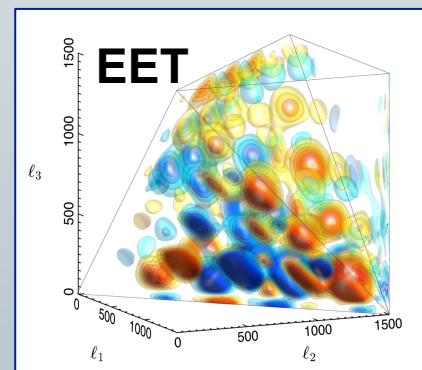
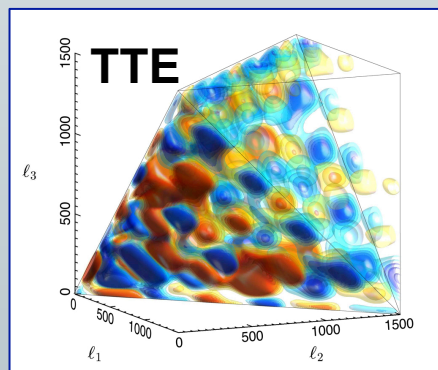
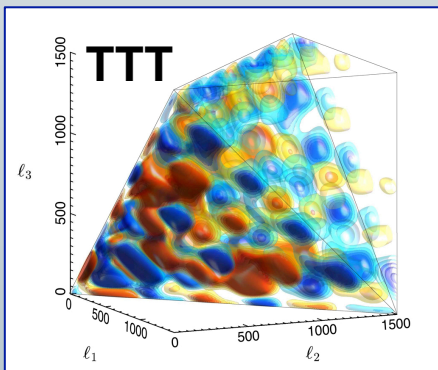
“Look elsewhere”
not accounted for

Features x Flat



Largest significance
obtained for
feature models with
“Flat” envelope

Best-fit Feature x Flat



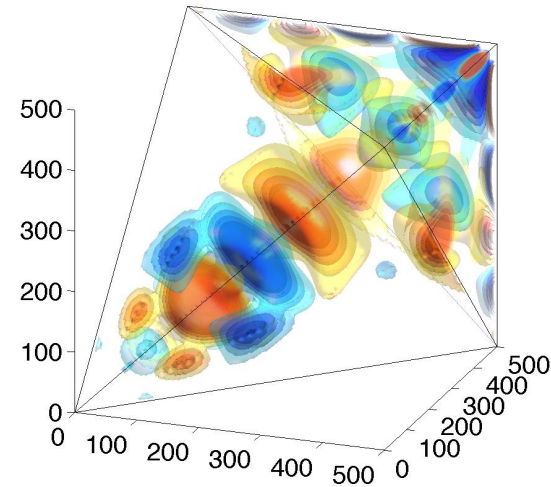
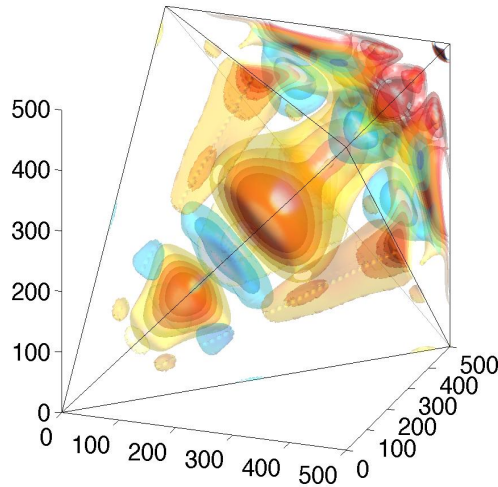
Planck vs WMAP

Planck

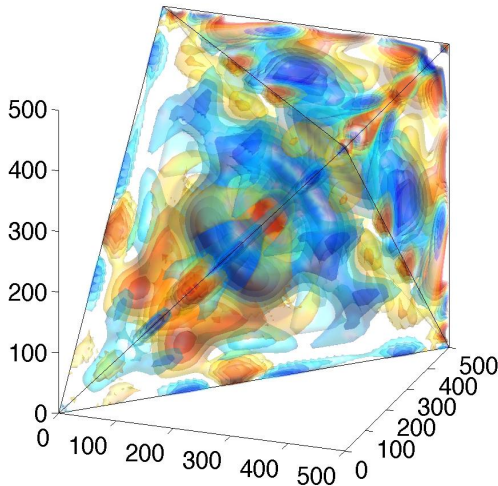
WMAP

M. Shiraishi, ML, J. Fergusson 2014

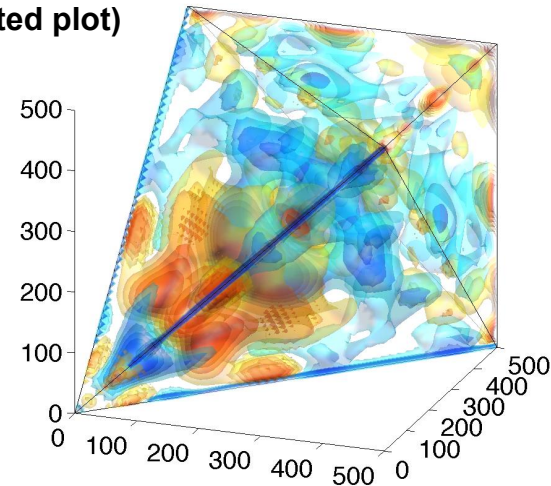
Parity-odd



Parity-even



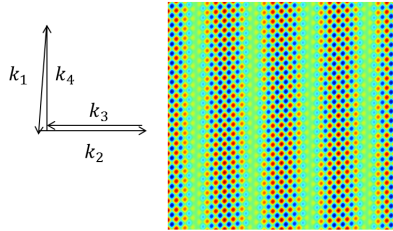
J Fergusson, ML, P. Shellard 2009, 2010
(updated plot)



Trispectrum

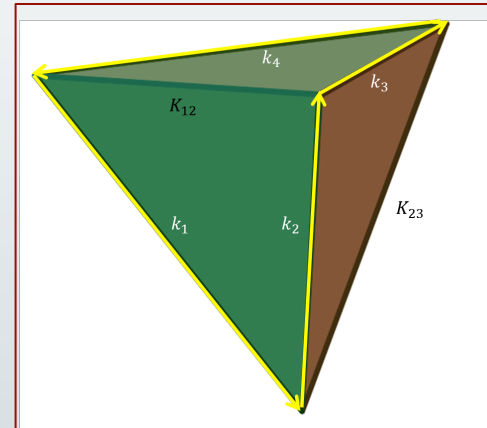
$$\langle \Phi(k_1) \Phi(k_2) \Phi(k_3) \Phi(k_4) \rangle \propto F(k_1, k_2, k_3, k_4, K_{12}, K_{23}) \delta(\vec{k}_1 + \vec{k}_2 + \vec{k}_3 + \vec{k}_4)$$

Diagonal squeezed trispectra $|k_1| \sim |k_2|, |k_3| \sim |k_4|, |k_1 + k_2| = |k_3 + k_4| \ll |k_2|, |k_3|$

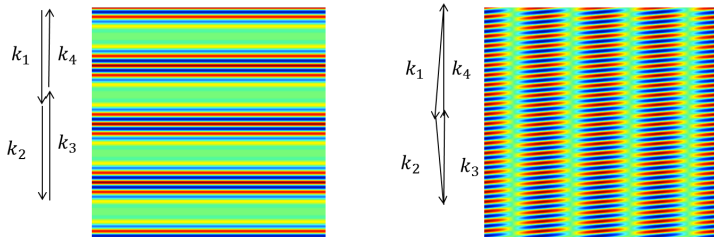


Diagonal squeezed trispectrum: τ_{NL}

$$\tau_{NL} < 2800 \quad (95\% \text{ C.L.})$$



Pictures from Lewis 2012

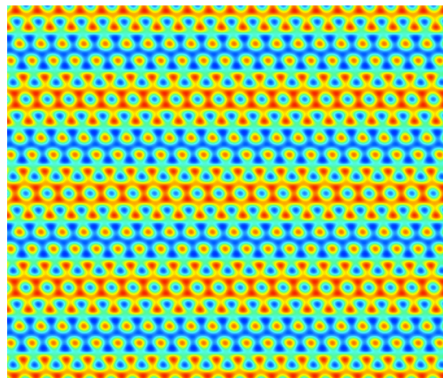
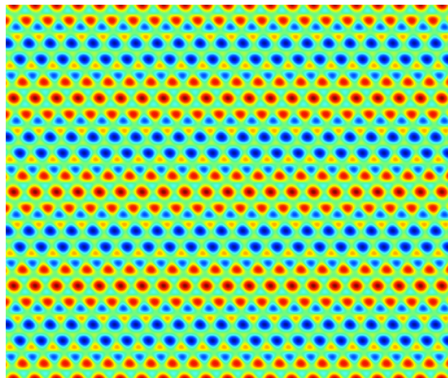
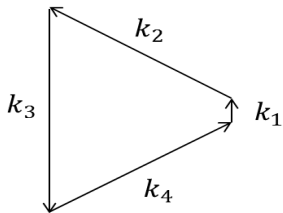


One-leg squeezed trispectra

$$|k_1| \ll |k_2| \sim |k_3| \sim |k_4|$$

Trispectrum > 0

Trispectrum < 0

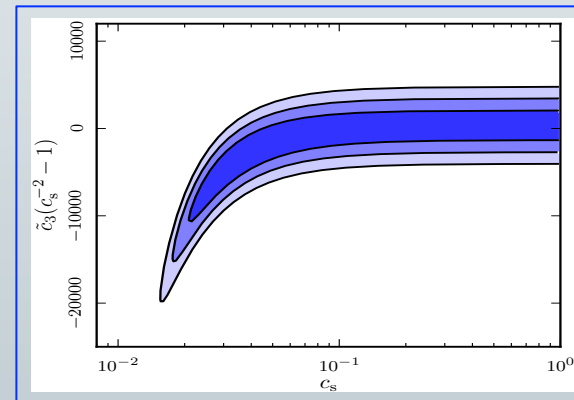
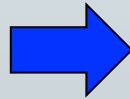
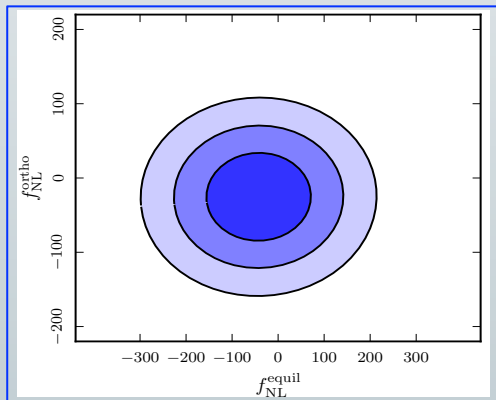


Leg squeezed trispectrum: g_{NL}

$$g_{NL}^{local} = (-9.0 \pm 7.7) \times 10^{-4}$$

Implications for inflation (examples)

- No evidence for primordial NG of the local, equilateral, orthogonal type. consistent with the simplest scenario: standard single-field slow roll.
- Other possibilities are however not ruled out. Constraints on f_{NL} are converted into constraints on relevant model parameters, for example:
 - Curvaton decay fraction $r_D > 19\%$ (from local f_{NL} , T+E)
 - Speed of sound in Effective Field Theory $c_s > 0.024$ (from equil. + ortho. f_{NL})



- DBI inflation: $c_s > 0.087$ (T+E)

Future prospects

What else can be done with the CMB bispectrum?

- ✓ Planck is very close to saturating the theoretical limit on f_{NL} sensitivity, which is achievable using CMB observations (a cosmic-variance-limited T+E full sky survey, up to $l \sim 3000$, could still improve by a factor ~ 2)
- ✓ The current level of sensitivity is amazing, but with these error bars we are still unable to directly probe predictions from standard single field models ($f_{\text{NL}} \sim 10^{-2}$!!), or rule out multi-field (e.g. curvaton, $|f_{\text{NL}}| > 5/4$)

For the required large improvements in sensitivity, we need other cosmological probes

LSS

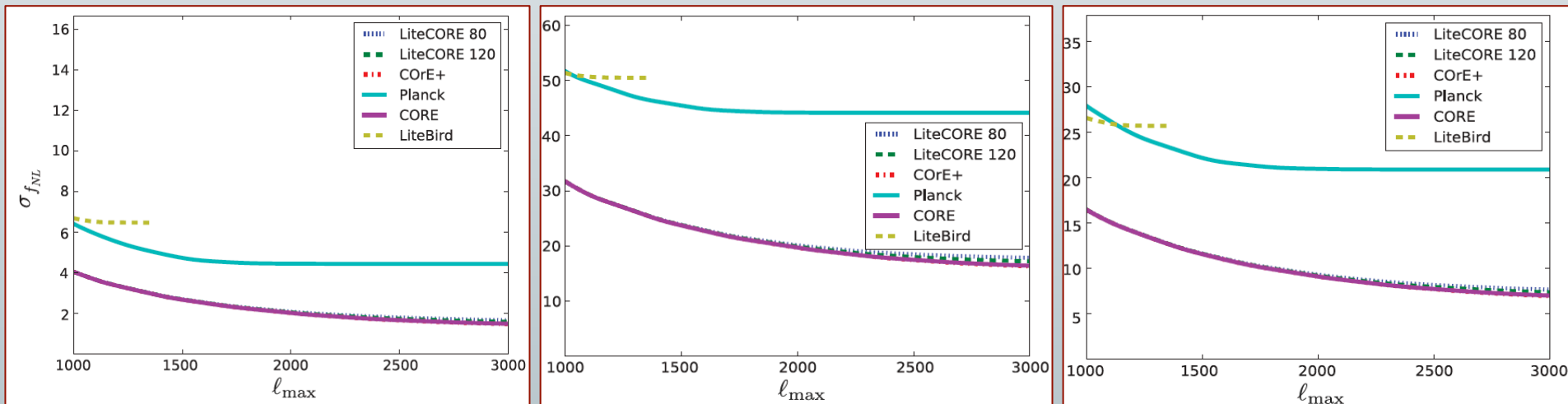
- ✓ Scale dependent halo bias (*local* $\Delta f_{\text{NL}} \sim 1$ with Euclid). Control of systematics will be crucial. *Both in galaxy surveys and CIB.*
- ✓ Bispectrum of galaxies. Sensitive to *all* shapes. *Needs small scales.*
Gravitational bispectrum, bias and other non-linear effects pose a serious challenge.

Other observables (futuristic)

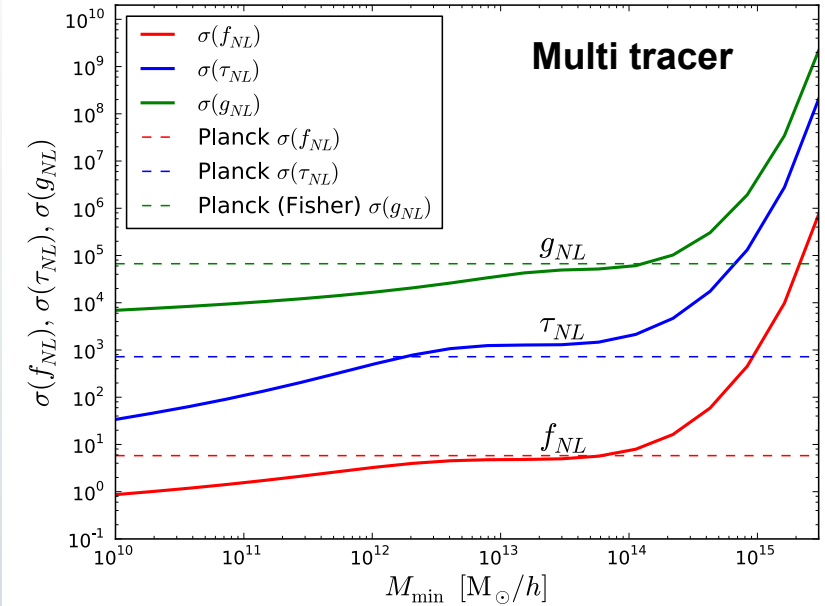
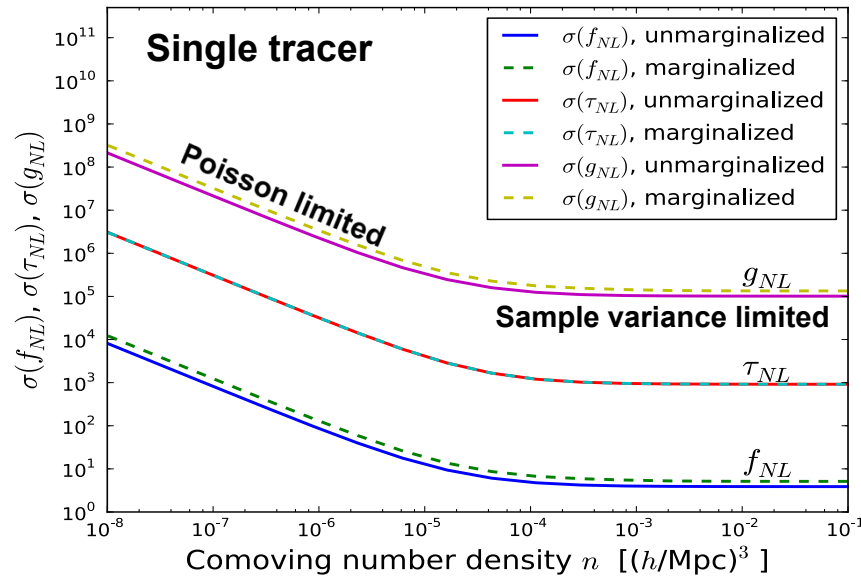
- ✓ CMB (μ -type) spectral distortions (only squeezed bispectra/trispectra)
- ✓ 21 cm bispectrum

CORE. CMB bispectrum forecasts

	LiteCORE 80	LiteCORE 120	CORE M5	COrE+	Planck 2015	LiteBIRD	ideal 3000
T local	4.5	3.7	3.6	3.4	(5.7)	9.4	2.7
T equilat	65	59	58	56	(70)	92	46
T orthog	31	27	26	25	(33)	58	20
T lens-isw	0.15	0.11	0.10	0.09	(0.28)	0.44	0.07
E local	5.4	4.5	4.2	3.9	(32)	11	2.4
E equilat	51	46	45	43	(141)	76	31
E orthog	24	21	20	19	(72)	42	13
E lens-isw	0.37	0.29	0.27	0.24		1.1	0.14
T+E local	2.7	2.2	2.1	1.9	(5.0)	5.6	1.4
T+E equilat	25	22	21	20	(43)	40	15
T+E orthog	12	10.0	9.6	9.1	(21)	23	6.7
T+E lens-isw	0.062	0.048	0.045	0.041		0.18	0.027



NG with LSS. 2-point function



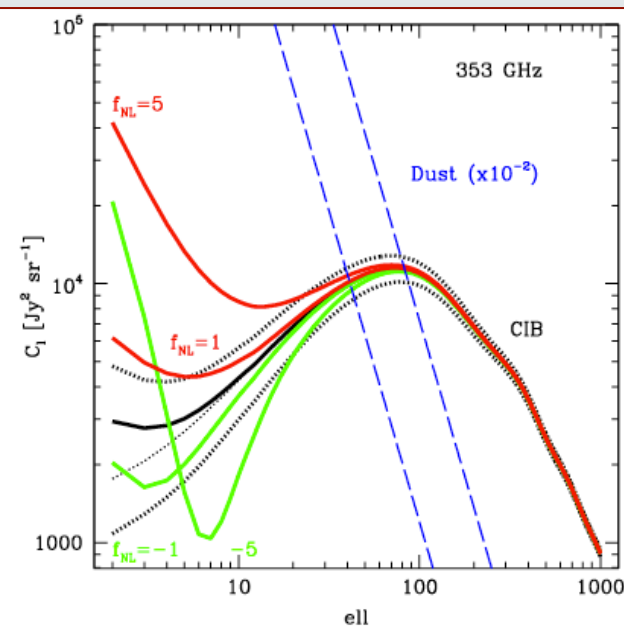
Ferraro and Smith 2014

$$\Delta b(k) = 2(b-1)f_{NL}\delta_c \frac{3\Omega_m}{2a g(a)r_H^2 k^2}$$

- Single tracer, $V = 25 \text{ Gpc}^3 h^{-3}$, statistical power \sim Planck
- Multi-tracer techniques have the power to reach $\sigma_{f_{NL}} \sim 1$ (local)
- Significant degeneracies between f_{NL} , g_{NL} , τ_{NL}

CIB power spectrum

- CIB power spectrum is integrated over a large volume. Ideal for scale dependent bias (Tucci et al. 2016)
- Seriously contaminated by dust, but future full-sky satellite B-mode experiments with many (high-)frequency channels allow very accurate component separation.



COrE+									$\sigma(f_{\text{NL}})$
ν [GHz]	220	255	295	340	390	450	520	600	
fwhm [arcmin]	3.82	3.29	2.85	2.47	2.15	1.87	1.62	1.40	
w^{-1} [$\text{Jy}^2 \text{sr}^{-1}$]	0.654	1.43	5.20	8.31	13.50	22.98	39.88	69.26	
Σ_{CIB}^2 [$\text{Jy}^2 \text{sr}^{-1}$]	–	8.04	–	47.3	–	212.	382.	–	1.6
COrE+ with <i>Planck</i>									
Σ_{CIB}^2 [$\text{Jy}^2 \text{sr}^{-1}$]	–	1.97	–	10.8	–	45.6	90.2	163.6	0.6
CORE									$\sigma(f_{\text{NL}})$
ν [GHz]	220	255	295	340	390	450	520	600	
fwhm [arcmin]	5.23	4.57	3.99	3.49	3.06	2.65	2.29	1.98	
w^{-1} [$\text{Jy}^2 \text{sr}^{-1}$]	0.29	0.57	0.77	1.08	2.16	3.55	6.2	11.0	
Σ_{CIB}^2 [$\text{Jy}^2 \text{sr}^{-1}$]	–	1.8	–	8.8	–	42.9	80.1	–	0.7
CORE with <i>Planck</i>									
Σ_{CIB}^2 [$\text{Jy}^2 \text{sr}^{-1}$]	–	1.03	–	5.2	–	23.3	43.9	68.9	0.34

(Tucci et al. 2016)

(Finelli et al. 2016)

NG with LSS. Bispectrum

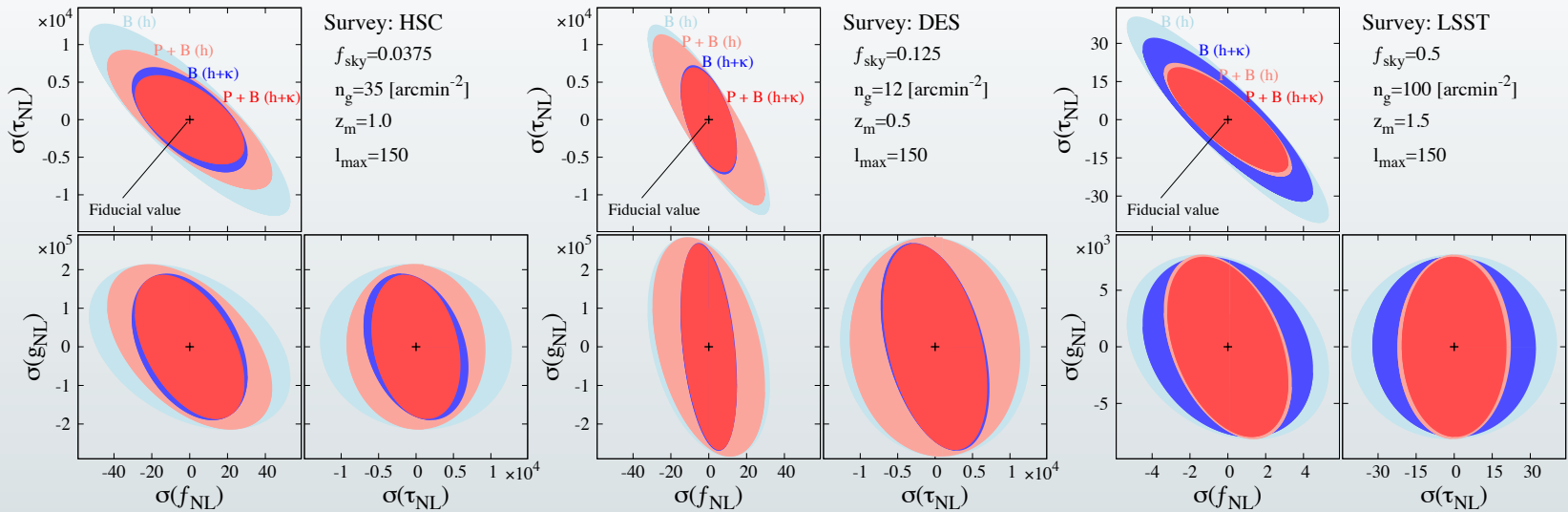
Sample	Power Spectrum		Bispectrum	
	$\sigma_{f_{\text{NL}}}$ bias float	$\sigma_{f_{\text{NL}}}$ bias fixed	$\sigma_{f_{\text{NL}}}$ bias float	$\sigma_{f_{\text{NL}}}$ bias fixed
BOSS	21.30	13.28	1.04 ^(0.65) _(2.47)	0.57 ^(0.35) _(1.48)
eBOSS	14.21	11.12	1.18 ^(0.82) _(2.02)	0.70 ^(0.48) _(1.29)
Euclid	6.00	4.71	0.45 ^(0.18) _(0.71)	0.32 ^(0.12) _(0.35)
DESI	5.43	4.37	0.31 ^(0.17) _(0.48)	0.21 ^(0.12) _(0.37)
BOSS + Euclid	5.64	4.44	0.39 ^(0.17) _(0.59)	0.28 ^(0.11) _(0.34)

Tellarini et al. 2016



- Fisher matrix forecast. Tree level bispectrum. Local NG initial conditions. In redshift space. Covariance between different triangles neglected (optimistic).
- Bispectrum could do better than power spectrum.
- $f_{\text{NL}} \sim 1$ achievable with forthcoming surveys?
- Many issues, e.g. full covariance, accurate bias model, GR effects, survey geometry, estimator implementation... Still, great potential: 3D vs 2D (CMB).

Galaxy + Lensing

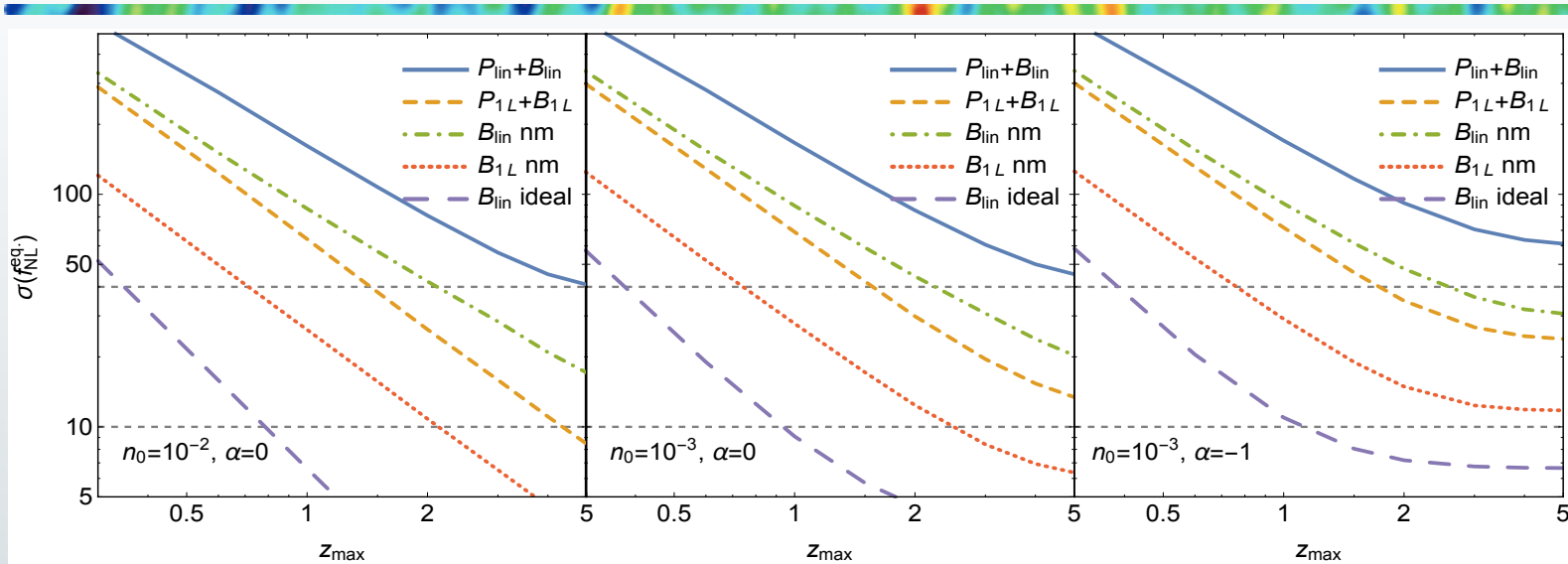


Hashimoto et al. 2016

Combining power spectra and bispectra, clustering and weak lensing, can help to break degeneracies between local NG parameters

	HSC	DES	LSST	current CMB
$\sigma(f_{\text{NL}})$	19 (9.2)	9.8 (5.2)	2.1 (0.89)	(5.1)
$\sigma(g_{\text{NL}})$	1.2×10^5 (7.1×10^4)	1.8×10^5 (1.0×10^5)	5.3×10^3 (3.8×10^3)	(1.4×10^5)
$\sigma(\tau_{\text{NL}})$	3.9×10^3 (2.1×10^3)	4.6×10^3 (2.5×10^3)	14 (6.2)	(1.4×10^3)

Equilateral NG. Theoretical uncertainties



Baldauf et al. 2016

- The LSS bispectrum allows in principle tight constraints also on non-local shapes e.g. equilateral
- Naive mode counting suggest $\sigma_{f_{NL}} \sim 1$ for equilateral might be achievable by pushing k_{max} high enough
- However, in the non-linear regime we have to model the gravitational bispectrum with high accuracy. Very challenging. Equilateral is more correlated than local to non-linear gravitational bispectrum, so bigger problem.

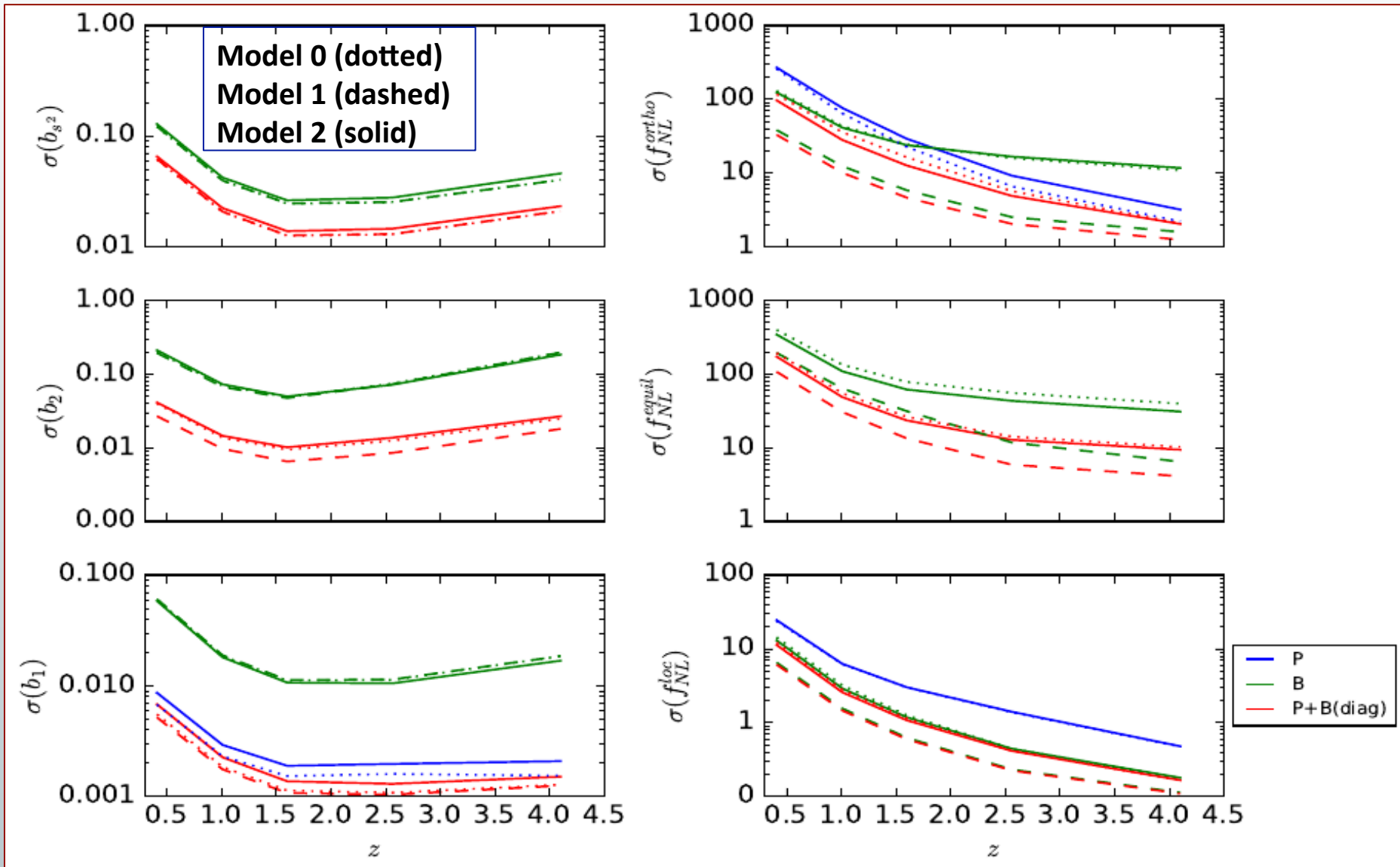
Radio surveys

- Wide radio surveys, reaching high- z can produce very interesting constraints in principle. High- z allows to reach higher k , while remaining in linear regime (but careful to theoretical errors)

Forecasts (D. Karagiannis, ML, A. Raccañelli, N. Bartolo, in prep.):

- Joint power spectrum/bispectrum prediction for local, equilateral,
- orthogonal + bias coefficients
- Use cross-correlation method between radio continuum surveys and spectroscopic datasets to derive redshift information on point sources (Schneider et al 2006, Newman et al 2008)
- Effective halo bias expansion up to 2nd order (Mirbabayi et al. 2014) parameters b_1 , b_2 , b_{s2} .
- Bivariate bias expansion for local shape
- $k_{\max} = 0.1/D(z)$
- Including trispectrum correction term (NG contrib. to tree-level bispectrum).
- RSD accounted for up to 2nd order (excluding trispectrum)
- Neglecting PB covariance
- Theoretical errors not included yet (should worsen forecast by a factor 3-4)
- **Model 0: Real space, no trispectrum. Model 1: Real space + trispectrum. Model 2: Redshift space, no trispectrum**

Forecasts: SKA



Model 0

	SKA ($1\mu Jy$)			ASKAP/EMU ($10\mu Jy$)		
	$\sigma(f_{NL}^{loc})$	$\sigma(f_{NL}^{equil})$	$\sigma(f_{NL}^{orth})$	$\sigma(f_{NL}^{loc})$	$\sigma(f_{NL}^{equil})$	$\sigma(f_{NL}^{orth})$
Power spectrum	0.44	-	2.0	0.94	-	5.43
Bispectrum	0.16	29	8.2	0.42	55.34	16.9
P+B (diagonal)	0.15	7.8	1.9	0.38	17	4.91

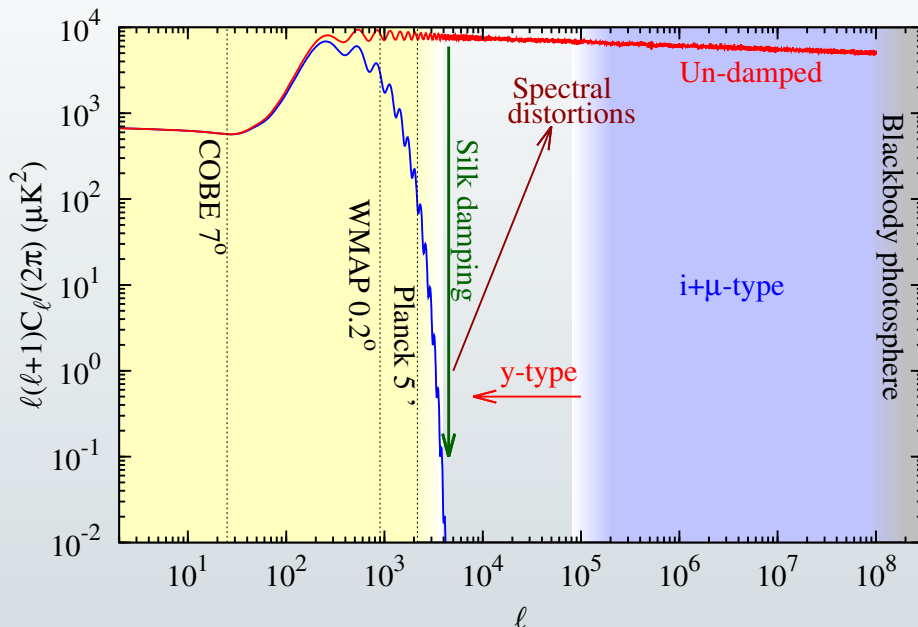
Model 1

	SKA ($1\mu Jy$)			ASKAP/EMU ($10\mu Jy$)		
	$\sigma(f_{NL}^{loc})$	$\sigma(f_{NL}^{equil})$	$\sigma(f_{NL}^{orth})$	$\sigma(f_{NL}^{loc})$	$\sigma(f_{NL}^{equil})$	$\sigma(f_{NL}^{orth})$
Power spectrum	0.44	-	2.0	0.94	-	5.43
Bispectrum	0.1	5.53	1.28	0.22	10.37	2.1
P+B (diagonal)	0.096	3.24	1.0	0.21	5.96	1.78

Model 2

	SKA ($1\mu Jy$)			ASKAP/EMU ($10\mu Jy$)		
	$\sigma(f_{NL}^{loc})$	$\sigma(f_{NL}^{equil})$	$\sigma(f_{NL}^{orth})$	$\sigma(f_{NL}^{loc})$	$\sigma(f_{NL}^{equil})$	$\sigma(f_{NL}^{orth})$
Power spectrum	0.44	-	2.97	0.96	-	7.73
Bispectrum	0.16	22.7	8.62	0.43	46.5	17.3
P+B (diagonal)	0.15	7.12	1.84	0.39	15.5	4.62

NG with CMB spectral distortions



CMB spectral distortions from acoustic wave dissipation probe a large range of scales, much smaller than CMB/LSS

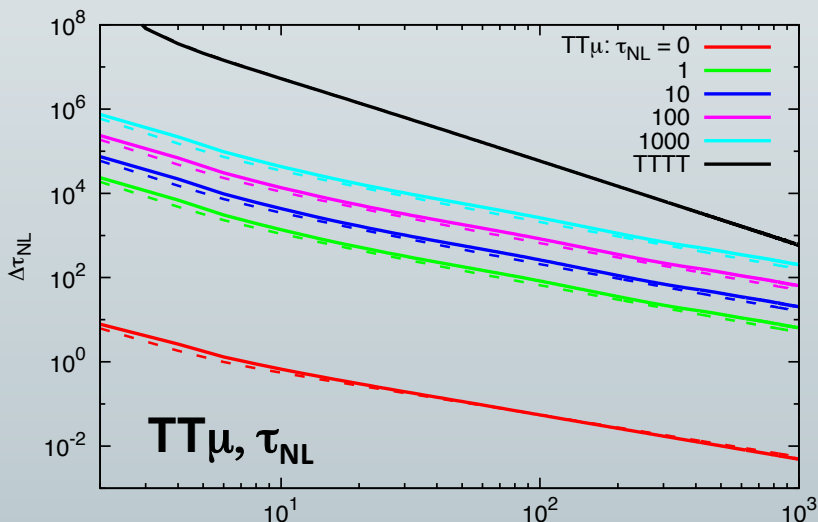
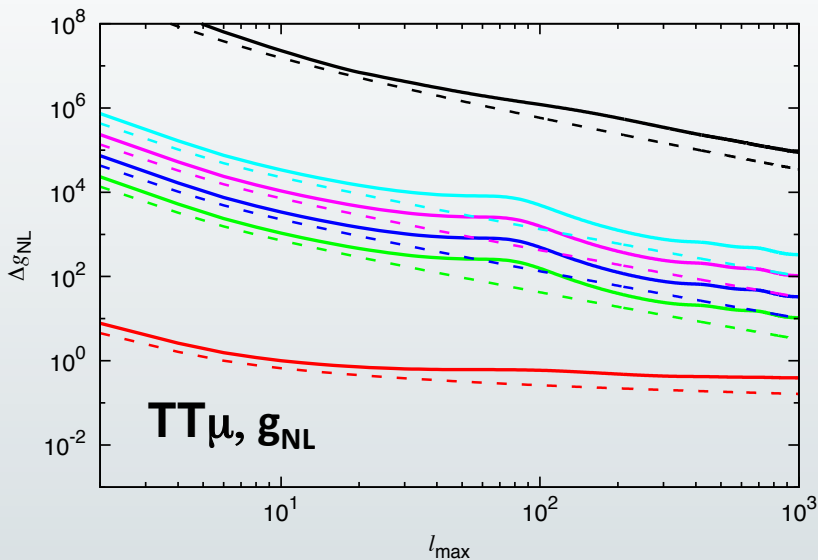
Many additional modes!

Kathri and Sunyaev 2013, arXiv: 1303.7212

If μ -anisotropies are measured ($\delta\mu \sim \Phi^2$):

- ✓ $T\mu$ correlation: primordial local f_{NL} (Pajer and Zaldarriaga 2013)
or other squeezed shapes, e.g. excited initial states (Ganc and Komatsu 2013)
- ✓ $\mu\mu$ correlation: primordial local trispectrum, τ_{NL}
- ✓ $TT\mu$ bispectrum: primordial local trispectrum, g_{NL}
(Bartolo, ML, Shiraishi 2016)

NG with CMB spectral distortions



For G initial conditions, dissipated power in small patches is isotropically distributed

If local NG \Rightarrow large scale modulation of small scale power \Rightarrow T μ correlations
(Pajer, Zaldarriaga 2013, Emami et al. 2015)



$$\Phi = \Phi_G + \Phi_{NG} = \Phi_G + f_{NL} \Phi_G^2,$$

$$\Phi_G = \Phi_S + \Phi_L \Rightarrow \Phi_{NG} = \Phi_S^2 + \Phi_L^2 + 2f_{NL} \Phi_S \Phi_L$$

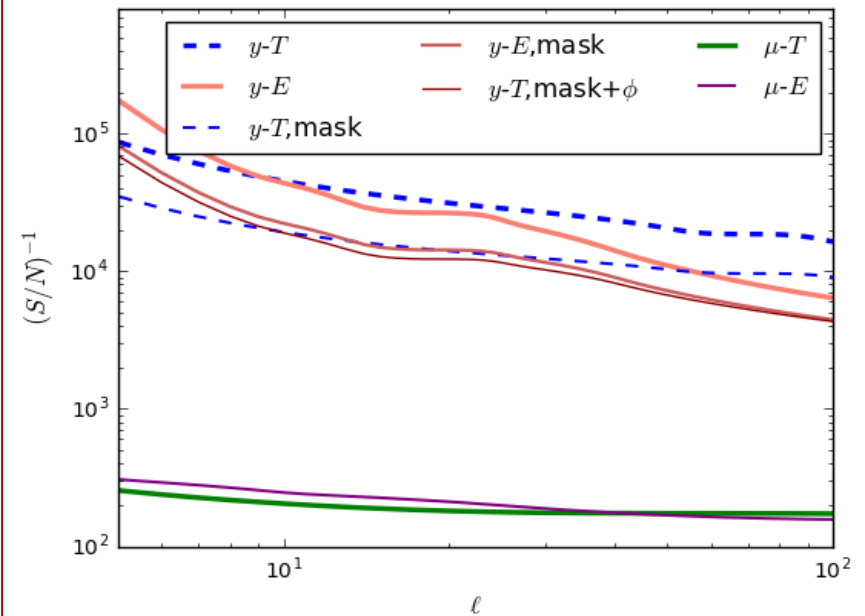
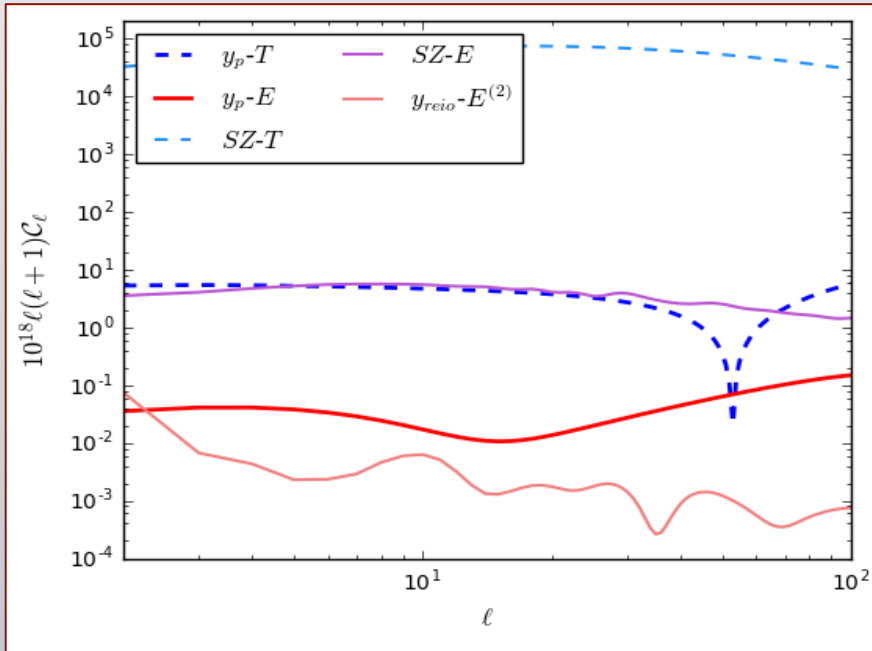
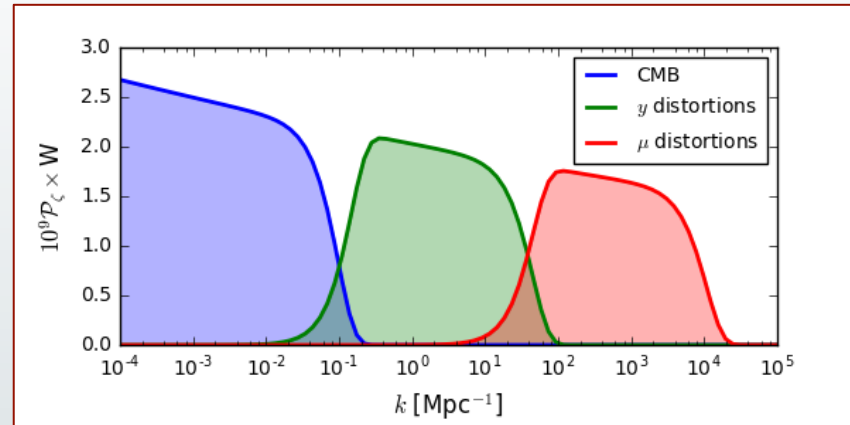
$$\Phi \propto \Phi_S (1 + 2f_{NL} \Phi_L) \Rightarrow \frac{\delta \langle \Phi^2 \rangle}{\Phi^2} = \frac{\delta \mu}{\mu} \sim 4f_{NL} \Phi_L$$

$$\Rightarrow \left\langle \frac{\delta T}{T} \right\rangle_L \frac{\delta \mu}{\mu} \propto f_{NL} C_\ell$$

Bartolo, ML, Shiraishi 2016

Scale dependent NG with μ and y

- T , μ and y -dist. probe different scales. Can be used to test NG scale dependence. (Biagetti et al. 2013, Emami et al. 2015)
- yT is strongly contaminated by SZ. Can improve by correlating with polarization (Ravenni et al. 2017 in prep.)

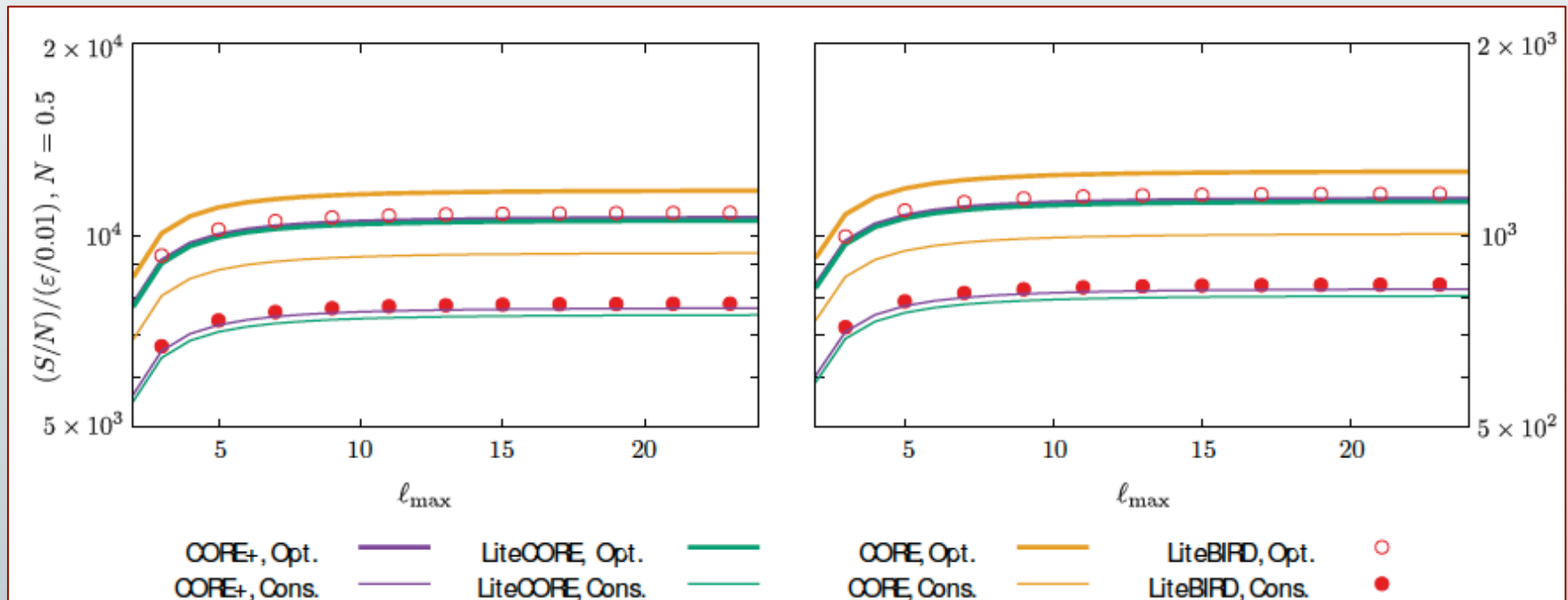


A. Ravenni, ML, N. Bartolo, M. Shiraishi in prep.

$$f_{\text{NL}}^{\mu}(\mu T) \gtrsim 175 \rightarrow f_{\text{NL}}^{\mu}(\mu T, E) \gtrsim 126 \quad f_{\text{NL}}^y(yT) \gtrsim 10^4 \rightarrow f_{\text{NL}}^y(yT, E) > 4300$$

Excited initial states

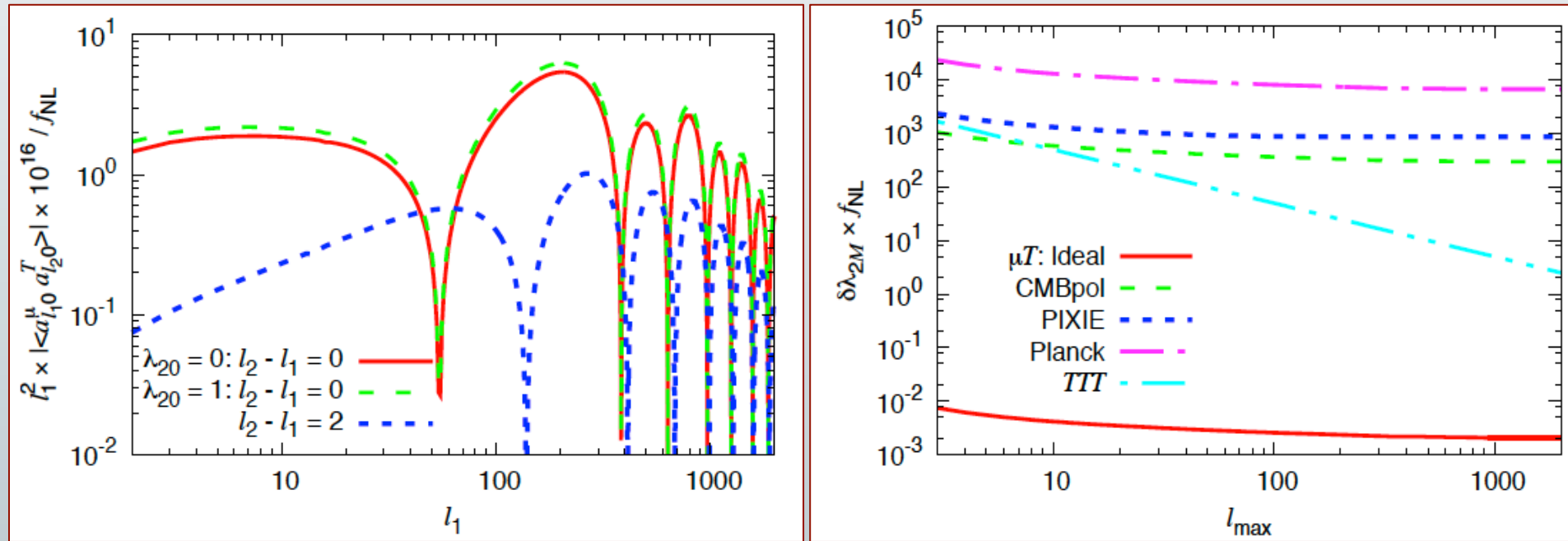
- Specific models with excited initial states predict enhanced signals in the squeezed limit (Agullo and Parker 2011).
- This can generate high S/N in μT tests (Ganc and Komatsu 2012)



Finelli et al. 2016

Anisotropic models

- The $\mu\mu$ auto-spectrum measures τ_{NL} type trispectra i.e. power spectrum modulation signals
- Anisotropic models produce distinctive off-diagonal entries in the $\mu\mu$ covariance

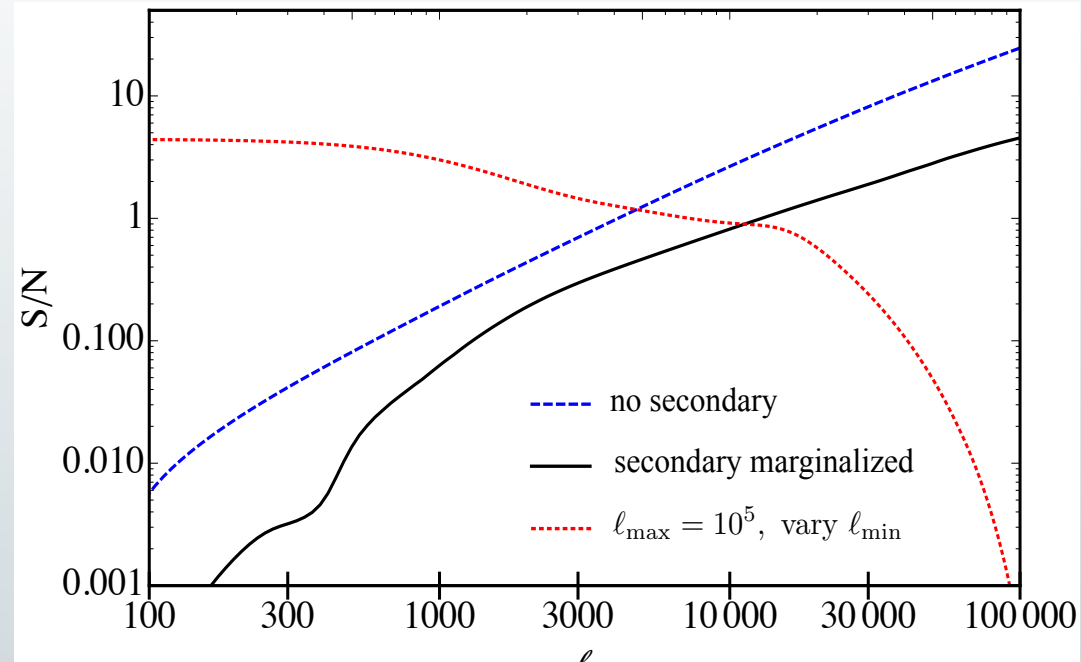


Shiraishi, ML, N. Bartolo 2015

21cm bispectrum

PNG type	$\sigma_{f_{\text{NL}}}$ (1 MHz)	$\sigma_{f_{\text{NL}}}$ (0.1 MHz)
Local	0.12	0.03
Equilateral	0.39	0.04
Orthogonal	0.29	0.03
$J = 1$	1.1	0.1
$J = 2$	0.33	0.05
$J = 3$	0.85	0.09

Munoz, Haimoud and Kamionkowski, 2015



- 21cm full-sky measurements reach very high $\ell_{\text{max}} \Rightarrow$ many modes and high S/N , even after marginalization of secondary effects + redshift tomography.

Conclusions

- Primordial NG probes interaction terms in the Inflationary action
Therefore it is a powerful test to discriminate between different scenarios
 - *Planck* NG results are consistent with predictions by the simplest inflationary models. However, we need more sensitivity to reach critical fNL thresholds. Local fNL=1 is the next goal
-
- CMB anisotropies have nearly saturated ideal limit
 - Next: scale-dependent halo bias and LSS bispectrum. 3-point function very challenging but sensitive to all shapes
 - CIB can be a very powerful local fNL probe, via large-scale power spectrum
 - Very powerful but futuristic: spectral distortions, 21 cm
 - Specific shapes are already interesting with spectral distortions.
 - Multiple approaches to local shape. Only bispectrum for the rest.

NG forecasts: future radio surveys

- λ We consider a SKA and ASKAP/EMU like surveys.
- λ Use cross-correlation method between radio continuum surveys and spectroscopic datasets to derive redshift information of point sources (Schneider et al 2006, Newman et al 2008).

ASKAP/EMU ($10\mu Jy$)			SKA ($1\mu Jy$)		
z	V	n	z	V	n
0.86	12.41	2.61	0.41	4.26	2.18
1.45	28.63	2.11	1.01	18.4	6.01
2.3	32.41	1.32	1.6	32.06	9.56
3.46	50.33	0.45	2.56	48.56	4.76
5.48	55.55	0.059	4.1	167.42	1.23

Table 2. The basic numbers for the two surveys considered here per redshift bin. The shell volume is in units of $(Gpc/h)^3$ and the mean number density in $10^{-4}(h/Mpc)^3$.

Bias

Effective halo bias expansion up to second order (N=2), of the form (Mirbabayi et al 2014)

$$\delta_h^L(\mathbf{q}) = \sum_{n=1}^N \frac{b_n^L}{n!} [\delta_R^{(1)}(\mathbf{q})]^n + \sum_{n=2}^N \frac{b_{s^n}^L}{n!} \text{Tr}[s_1^n(\mathbf{q})]$$

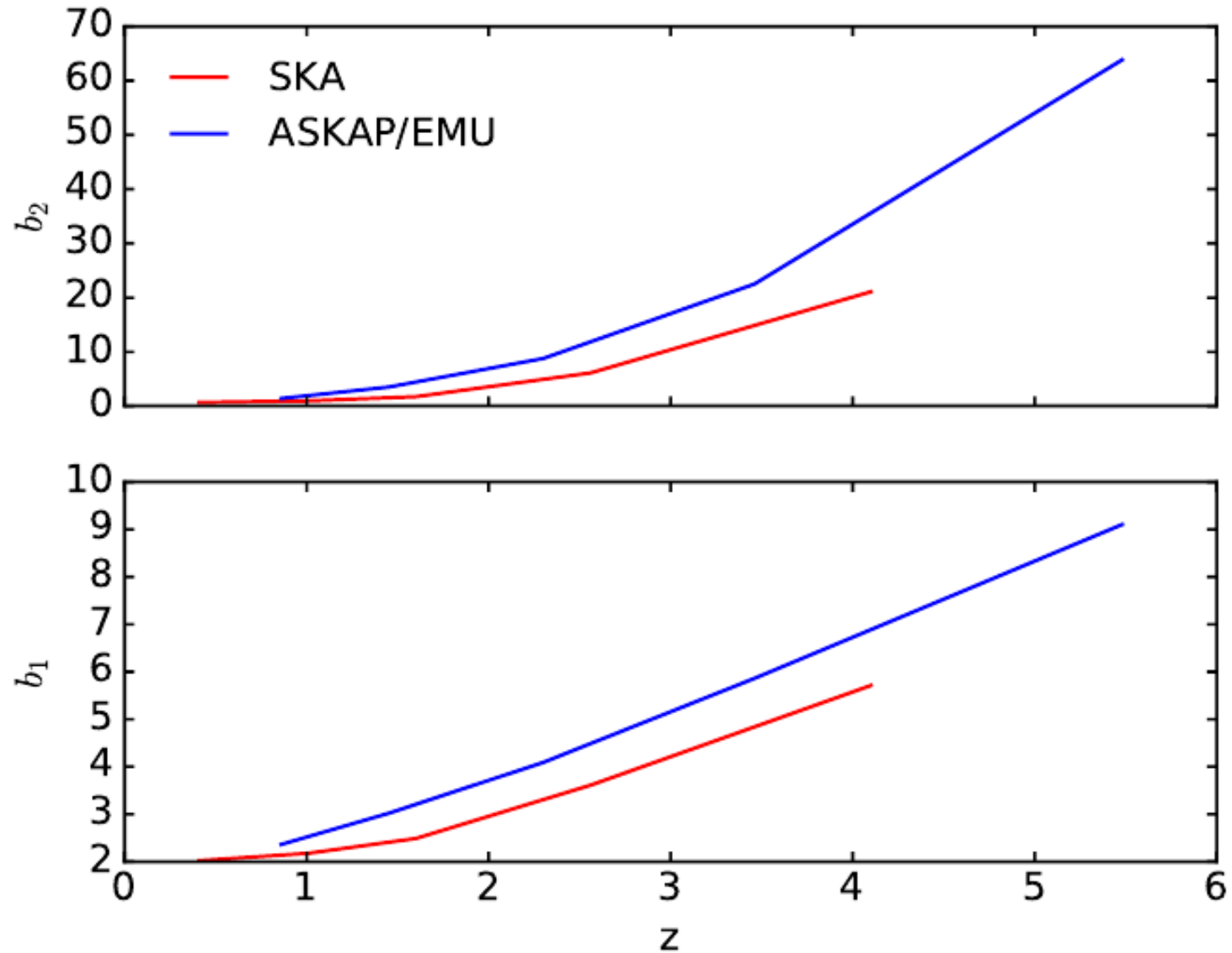
Stay in large-intermediate scales, hence we exclude stochastic bias.

Second part of the expansion are the tidal field terms. For n=2 the tidal term bias is a simple function of linear bias.

Use a weighted average with respect to a simple HOD to derive galaxy bias from the PBS halo model.

$$\langle N(M) \rangle = \begin{cases} 1 + \frac{M}{M_1} \exp\left(-\frac{M_{cut}}{M}\right), & \text{if } M \geq M_{min} \\ 0, & \text{otherwise,} \end{cases}$$

Bias



Model

We use the fisher matrix formalism to derive prediction on assumed free parameters from the two and three point statistics.

In fourier space power spectrum and bispectrum of the galaxies is:

$$P_g(k, z) = (b_1 + \delta b_1(f_{NL}) + \Delta b_1(k, f_{NL}))^2 P_m^L(k, z)$$

$$\begin{aligned} B_g(\mathbf{k}_1, \mathbf{k}_2, \mathbf{k}_3, z) = & b_1^3 (B_G(k_1, k_2, k_3, z) + B_I(k_1, k_2, k_3, z)) \\ & + \frac{b_1^2 b_2}{2} \left(2(P_m^L(k_1, z) P_m^L(k_2, z) + 2\text{perm}) \right. \\ & + \left. \left(\int \frac{d^3 q}{(2\pi)^3} T(\mathbf{k}_1, \mathbf{k}_2, \mathbf{q}, \mathbf{k}_3 - \mathbf{q}) + 2\text{perm} \right) \right) \\ & + b_{s^2} b_1^2 \left(2(S_2(\mathbf{k}_1, \mathbf{k}_2) P_m^L(k_1, z) P_m^L(k_2, z) + 2\text{perm}) \right. \\ & + \left. \left(\int \frac{d^3 q}{(2\pi)^3} S_2(\mathbf{q}, \mathbf{k}_3 - \mathbf{q}) T(\mathbf{k}_1, \mathbf{k}_2, \mathbf{q}, \mathbf{k}_3 - \mathbf{q}) + 2\text{perm} \right) \right) \end{aligned}$$

For the trispectrum term in bispectrum we consider only the non-Gaussian contribution to the tree level trispectrum.

We exclude primordial trispectrum since $O(f_{\text{NL}}^2)$.

For the local PNG we consider a bivariate bias expansion (Giannantonio et al 2009) .

Finally we test the effect of RSD up to second order in the predicted variables, excluding trispectrum contributions from the bispectrum.

The Fisher matrix for the two correlators will be:

$$F_{\alpha\beta}^P = \sum_{k=k_f}^{k_{\max}} \frac{\partial P_g(k)}{\partial p_\alpha} \frac{\partial P_g(k)}{\partial p_\beta} \frac{1}{\Delta P^2}$$

$$F_{\alpha\beta}^B = \sum_{k_1 \leq k_2 \leq k_3 = k_f}^{k_{\max}} \frac{\partial B_g(k_1, k_2, k_3)}{\partial p_\alpha} \frac{\partial B_g(k_1, k_2, k_3)}{\partial p_\beta} \frac{1}{\Delta B^2}$$

Fisher matrix predictions

- We consider as free parameters $p=\{f_{\text{NL}}, b_1, b_2, b_s\}$ and for the RSD model $p=\{f_{\text{NL}}, b_1, b_2, b_s, \sigma_p, f\}$.
- $k_{\text{max}}=0.1/D(z)$, $k_{\text{min}}=k_f$
- For the powerspectrum bispectrum joint predictions we neglect off-diagonal terms in the covariance,
- We neglect for now theoretical errors, although they can increase the errors 3-4 times.

$$F_{\alpha\beta}^{P+B} = F_{\alpha\beta}^P + F_{\alpha\beta}^B$$

- 3 models for the galaxy bispectrum are used for the prediction.

1)Model 0: Redshift space bispectrum (monopole only) excluding trispectrum loop correction.

2)Model 1: Redshift space bispectrum (monopole only) including trispectrum correction.

3)Model 2: Redshift space bispectrum (RSD 2nd order), without including trispectrum.

Fisher matrix predictions

Model 0

	SKA ($1\mu Jy$)			ASKAP/EMU ($10\mu Jy$)		
	$\sigma(f_{NL}^{loc})$	$\sigma(f_{NL}^{equil})$	$\sigma(f_{NL}^{orth})$	$\sigma(f_{NL}^{loc})$	$\sigma(f_{NL}^{equil})$	$\sigma(f_{NL}^{orth})$
Power spectrum	0.44	-	2.0	0.94	-	5.43
Bispectrum	0.16	29	8.2	0.42	55.34	16.9
P+B (diagonal)	0.15	7.8	1.9	0.38	17	4.91

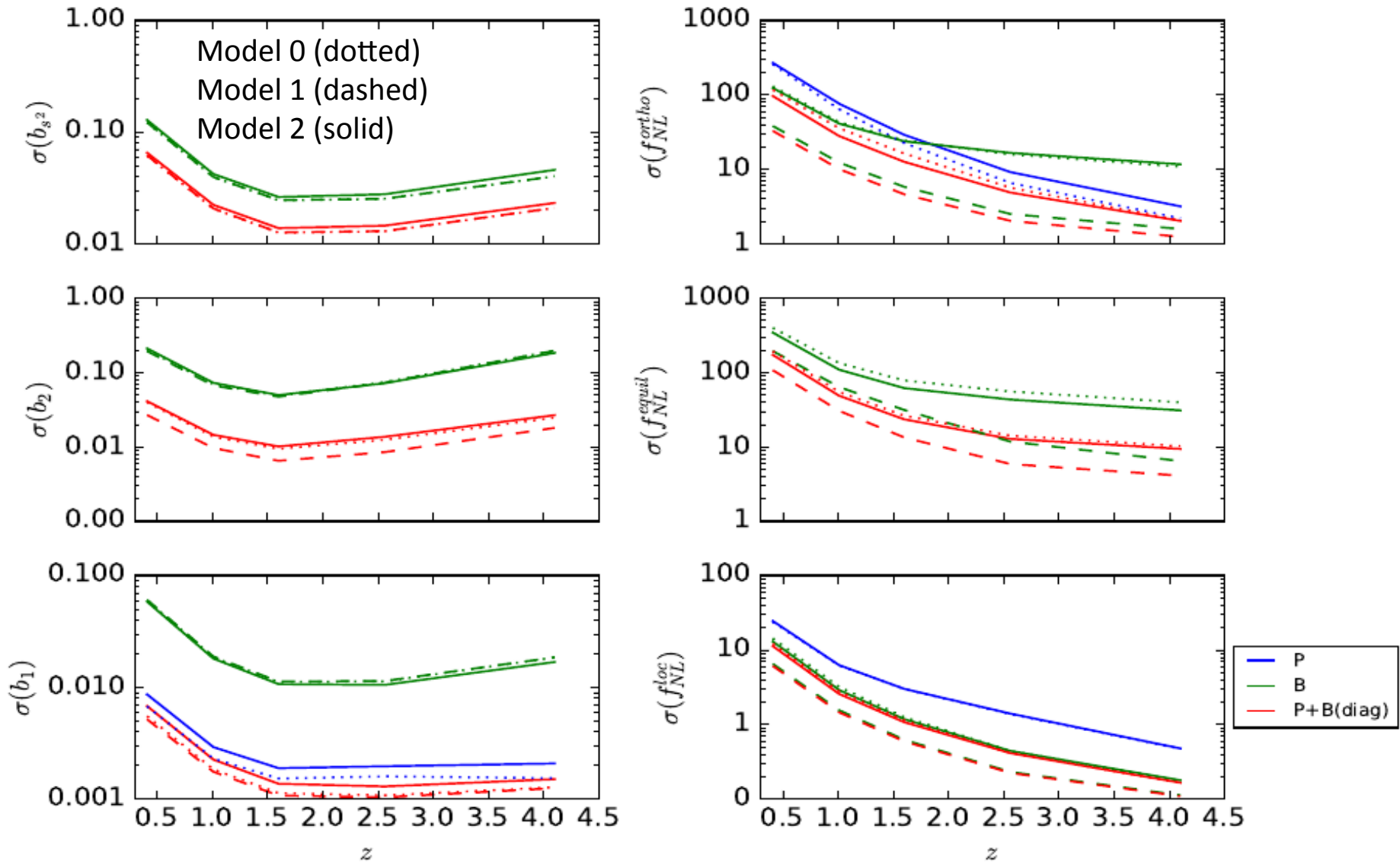
Model 1

	SKA ($1\mu Jy$)			ASKAP/EMU ($10\mu Jy$)		
	$\sigma(f_{NL}^{loc})$	$\sigma(f_{NL}^{equil})$	$\sigma(f_{NL}^{orth})$	$\sigma(f_{NL}^{loc})$	$\sigma(f_{NL}^{equil})$	$\sigma(f_{NL}^{orth})$
Power spectrum	0.44	-	2.0	0.94	-	5.43
Bispectrum	0.1	5.53	1.28	0.22	10.37	2.1
P+B (diagonal)	0.096	3.24	1.0	0.21	5.96	1.78

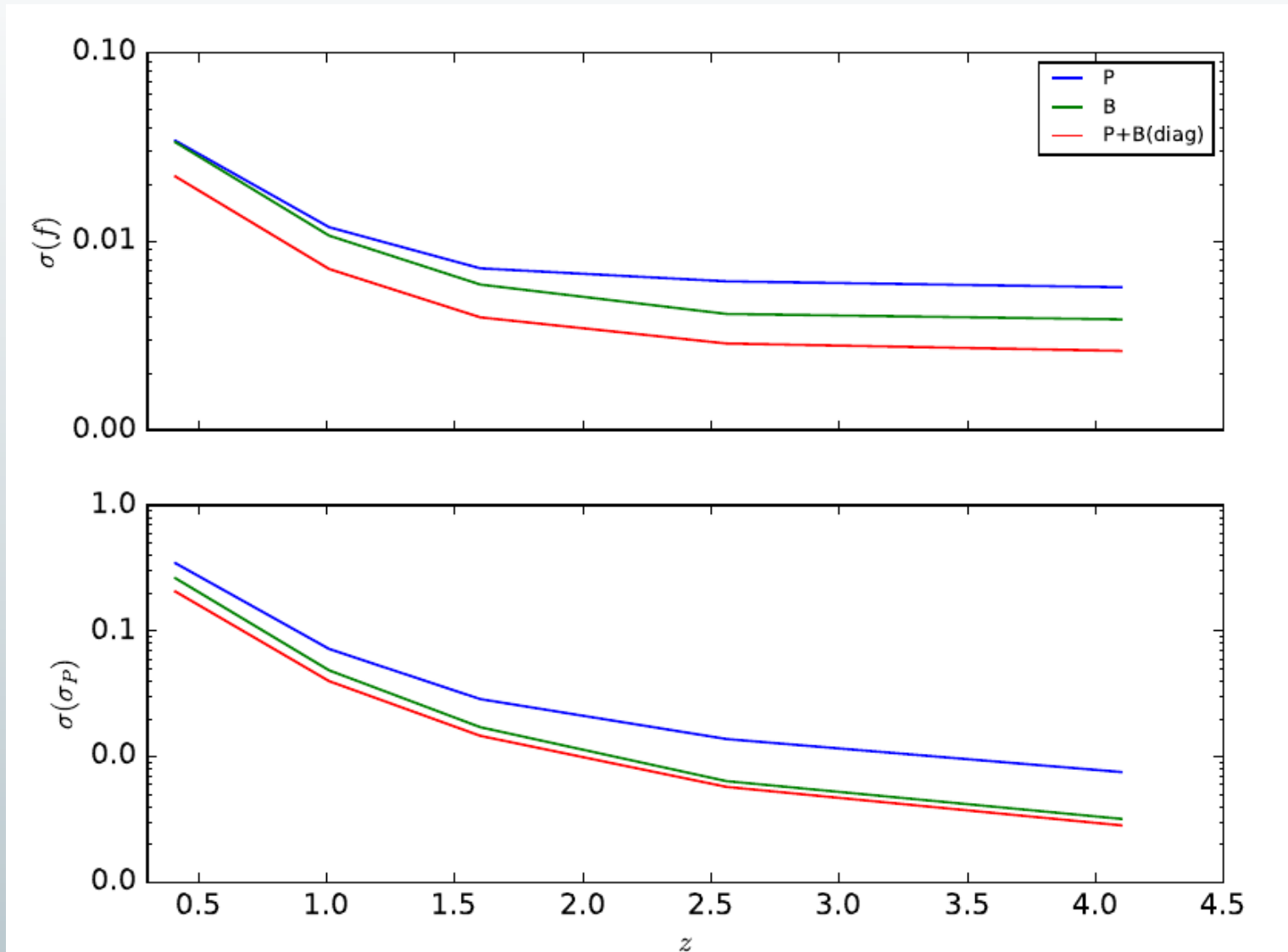
Model 2

	SKA ($1\mu Jy$)			ASKAP/EMU ($10\mu Jy$)		
	$\sigma(f_{NL}^{loc})$	$\sigma(f_{NL}^{equil})$	$\sigma(f_{NL}^{orth})$	$\sigma(f_{NL}^{loc})$	$\sigma(f_{NL}^{equil})$	$\sigma(f_{NL}^{orth})$
Power spectrum	0.44	-	2.97	0.96	-	7.73
Bispectrum	0.16	22.7	8.62	0.43	46.5	17.3
P+B (diagonal)	0.15	7.12	1.84	0.39	15.5	4.62

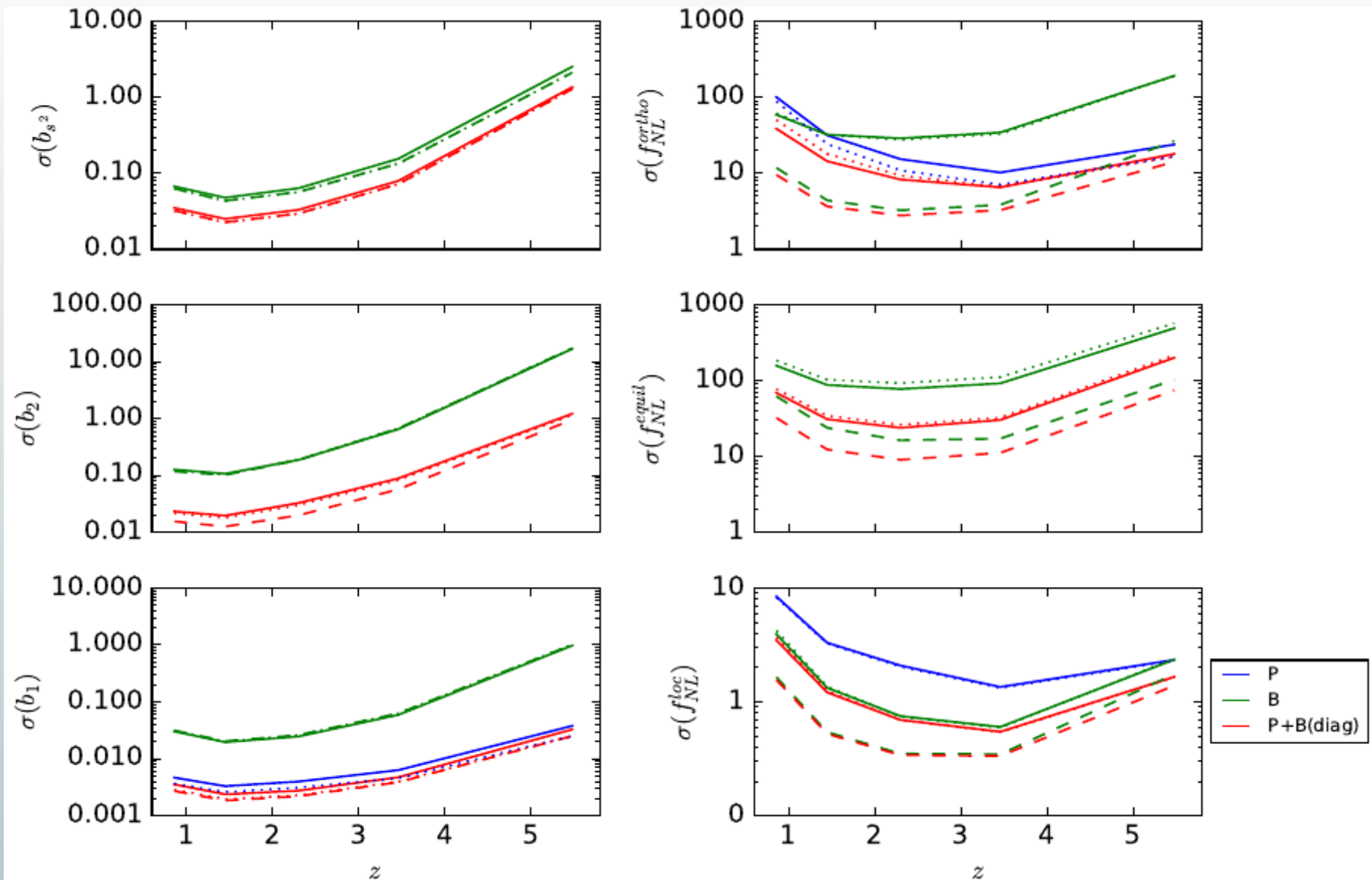
Predictions for SKA



Predictions for SKA



Predictions for ASKAP/EMU



Predictions for ASKAP/EMU

